Coordination Chemistry Reviews 518 (2024) 216059

Contents lists available at ScienceDirect

Coordination Chemistry Reviews

journal homepage: www.elsevier.com/locate/ccr

Review

Metal-organic frameworks for the diagnosis and treatment of Alzheimer's disease: Current status and perspectives

Guimei Zhang [a,b,1], Yanxin Shen [a,b,1], Joshua Phipps [c], Li Sun [a,b,*], Shengqian Ma [c,*]

[a] Department of Neurology and Neuroscience Center, The First Hospital of Jilin University, Jilin University, Xinmin Street #1, 130021 Changchun, China
[b] Cognitive Center, Department of Neurology, The First Hospital of Jilin University, Jilin University, Xinmin Street #1, 130021 Changchun, China
[c] Department of Chemistry, University of North Texas, 1508 W Mulberry St, Denton, TX 76201, United States

ARTICLE INFO

Keywords:
Alzheimer's disease
Metal–organic framework
Diagnosis
Treatment

ABSTRACT

Alzheimer's disease (AD) is a major cause of dementia and exhibits a complex and diverse pathogenesis with limited clinical treatment options, especially for patients in advanced stages. Therefore, early prevention, diagnosis, and treatment of AD are of great importance. Due to their excellent functionality in biosensing, bioimaging, and drug delivery, metal–organic frameworks (MOFs) have attracted extensive attention in recent years arising from their potential in AD diagnosis and therapy. They are a novel class of materials featuring highly controllable pore structures and surface chemistry with applications in a variety of areas such as adsorption, separation, catalysis, and drug delivery. This review provides an outline for the applications and potential toxicity of MOFs and detailed studies related to the diagnosis and treatment of AD utilizing MOFs. These works include diagnostic studies in which MOFs specifically detect β-amyloid, phosphorylated tau proteins, and neurotransmitters, as well as therapeutic studies in which MOFs are combined with biologically active molecules such as enzymes or nucleic acid sequences to target brain tissue or diseased nerve cells. With this review, we aim to broaden the use of MOFs in the diagnosis and treatment of AD and provide new research directions for clinical interventions in AD.

1. Introduction

Dementia is a significant public health issue affecting populations worldwide, with an annual incidence of nearly 10 million cases and is estimated to reach a global prevalence of over 152 million cases by 2050 [1]. Alzheimer's disease (AD) is the most common form of dementia, accounting for 60–80 % of all cases [2]. Despite prolonged efforts to overcome this disease [3], conventional preventive and therapeutic strategies that delay cognitive decline and Alzheimer's as well as other dementia-related disorders remain limited. Consequently, the World Health Organization has launched a global action plan that is currently aimed at addressing dementia as a public health priority, urging countries to implement interventions to prevent or delay cognitive decline and dementia [1]. Additionally, the Lancet Commission has identified 12 modifiable risk factors that account for approximately 40 % of global dementias [4], and has called for education and awareness-raising campaigns for patients and caregivers by emphasizing lifestyle changes, care management, and education to potentially prevent or delay dementia.

AD is a complex and multifactorial disease with genetic, pathogenic, and mechanistic heterogeneity, and its high incidence and incurability make it one of the biggest societal healthcare challenges. The clinical manifestation of AD includes progressive decline in memory and other cognitive functions, with two major pathological hallmarks: extracellular amyloid-beta (Aβ) plaques formed from Aβ peptides and intracellular neurofibrillary tangles (NFTs) formed from hyperphosphorylated or abnormally phosphorylated tau aggregation. In addition to the neurotoxicity stemming from Aβ and highly phosphorylated tau, chronic inflammation caused by over-activated microglia and microglia-related gene expression dysregulation [5], immune system aging [6], and neuroimmune axis [7] malfunction have also been implicated in the development of AD. Over the past two decades, therapeutic approaches targeting Aβ and highly phosphorylated tau have yielded limited efficacy with no significant evidence of slowing disease progression,

* Corresponding authors at: Department of Neurology and Neuroscience Center, The First Hospital of Jilin University, Jilin University, Xinmin Street #1, 130021 Changchun, China (L. Sun). Department of Chemistry, University of North Texas, 1508 W Mulberry St, Denton, TX 76201, United States (S. Ma).
E-mail addresses: sunli99@jlu.edu.cn (L. Sun), Shengqian.Ma@unt.edu (S. Ma).
[1] Guimei Zhang and Yanxin Shen contributed equally to this work.

https://doi.org/10.1016/j.ccr.2024.216059
Received 20 March 2024; Accepted 25 June 2024
Available online 4 July 2024

prompting researchers to continually reassess and explore alternative strategies.

A significant hurdle for effective treatment arises due to the complex and multi-organ system of the human body, where drugs may undergo a series of pharmacokinetic processes upon entering and making their way to the target site. This results in an increased risk of degradation before reaching target organs or cells. Furthermore, the blood–brain barrier (BBB) significantly restricts the permeability of drugs, limiting their precision targeting and ability to achieve an effective therapeutic concentration. These challenges have created a pressing need for the development of a suitable and reliable platform for visualizing drug release that could aid in elucidating mechanisms of cellular uptake and guiding new drug design. Metal-organic frameworks (MOFs) have been identified as a prospective solution to overcome these challenges. MOFs have regular arrangements of large cavities and crystalline structures constructed from organic ligands serving as scaffolds and metal ions as nodes [8,9]. In recent years, MOFs have emerged as cutting-edge hybrid materials in the field of biomedicine, eliciting enthusiastic attention from medical researchers. Despite MOFs exhibiting slightly less stability in certain aspects compared to inorganic materials such as silica and carbon structures, as well as organic materials like liposomes and polymers [10], particularly in terms of long-term stability in aqueous solutions, this may present a challenge to their applications in drug delivery and imaging. Moreover, the complex preparation process of MOFs, involving multiple steps and precise synthesis conditions, results in relatively high production costs. However, despite these potential drawbacks of MOFs, with the rapid advancements in material synthesis technologies, MOFs continue to demonstrate outstanding advantages among a myriad of materials. Especially in the field of drug delivery, the innovative applications of MOFs have greatly propelled the prosperity of the medical market. This is mainly attributed to several significant advantages of MOFs: 1) their tunability and flexible modification endow them with unparalleled diversity, constructing a library of MOFs materials comprising thousands of different structures and functions [11]; 2) their unique weak coordination bond characteristics make MOFs easily biodegradable and allow for precise degradation according to actual requirements, effectively addressing the challenge of the difficult degradation of traditional inorganic materials [10]; 3) the enhanced thermal and chemical stability of MOFs ensures their potential for repetitive use in medical applications [12]; 4) with high porosity, diverse pore shapes, and extensive surface area, MOFs provide an ideal platform for efficient loading and encapsulation of drugs, leading to a significant enhancement in drug delivery efficiency, surpassing the limitations of organic materials in loading capacity [13]; 5) MOFs enable responsive drug release through external stimuli (such as light, temperature, pH, etc.) and, through meticulous design, facilitate targeted delivery of genes and drugs, enhancing therapeutic efficacy and minimizing side effects [14,15]; 6) MOFs also exhibit good biocompatibility, ensuring their biological safety in clinical applications.

This review provides a detailed overview of the applications and potential toxicity concerns when using MOFs in the biomedical field. Additionally, the review summarizes the latest research advances in the use of MOFs for body fluid detection and drug delivery in AD, aiming to provide new research directions and insights for AD diagnosis and treatment.

2. Introduction to MOFs and their potential for biomedical applications

The basic building blocks of MOF materials are inorganic metal ions and organic ligands. The metal ions act as inorganic linkage points for the organic ligands and as they extend and connect to one another they form metal ion clusters called secondary building units (SBU) [16]. These SBUs then extend further to create larger frameworks. Strictly speaking, MOFs can be classified as a nanoscale porous material, which not only possesses the conventional structural characteristics of porous materials, but also exceeds the properties of conventional porous materials to a certain extent. These characteristics include: (1) the variability of metal centers as well as organic ligands which allow for diversity and specificity of MOF materials; (2) a new generation of zeolite materials; (3) low skeleton density; (4) large specific surface area; (5) adjustable pore structure and functional modification; and (6) a large number of unsaturated metal active sites (8). These characteristics provide MOFs with extensive functionalities and capabilities for a wide range of applications. Specifically, they have garnered significant interest in the fields of gas adsorption, catalysis, separation and enrichment, and drug delivery [11]. Catalytic reactions are made possible in part by the large number of unsaturated metal sites exposed outside and within the material that can be utilized for specific chemical reactions. As more of these active sites are exposed, there is a direct correlation to an increase in the kinetics of the related chemical reactions [17,18]. The versatility of MOF structures and the diversity of material properties are not only related to metal ions and organic ligands, but are also inextricably linked to the synthesis conditions of MOFs. These synthesis methods may include the use of evaporative solvent, diffusion, hydrothermal or solvothermal, ultrasound and microwave strategies [16]. Different functional MOF materials require specific material synthesis methods which, when adjusted, can yield a MOF with a different topology.

Over the last 20 years, an increasing number of specific structures of MOFs have been synthesized. A review by Furukawa et al., published in Science in 2013 [19], provides a detailed summary of progress in the synthesis of MOF materials. As of 2020, the Cambridge Structural Database has reported over 100,000 MOFs with different geometries, sizes and functions [20,21]. MOF materials have become a mainstream research topic due to their practical use and potential in future applications. In order to meet the practical demands of MOFs, it is imperative to enhance their properties and introduce new functionalities. This has encouraged and focused research on innovative approaches such as functionalizing MOF materials or combining them with other functionalized materials to create composite MOF materials. These composites effectively combine the advantages of MOF structural adaptability, flexibility, high porosity, and ordered crystal pores, with the unique optical, electrical, magnetic, and catalytic properties of different functionalized materials. This has resulted in new physical and chemical properties and improved material performance that cannot be achieved by individual components [22]. To date, MOFs have been successfully combined with nanoparticles (NPs), carbon-based materials, polymers, biomolecules, and other materials to form complex MOF-based systems [23–26]. This approach bridges the gap and extends the range of applications of single MOF materials.

More importantly, the size and density of various components of MOF composites have been successfully reduced to the nanoscale through innovations in materials synthesis techniques. This reduction presents a unique opportunity to enhance composite properties and expand their applications in biomedical fields [24]. The applications of nanotechnology in the biomedical field have facilitated the rapid development of NPs in biosensors and drug/non-drug delivery systems (Fig. 1). However, for successful translation from pre-clinical to clinical applications, such as drug and non-drug delivery based on MOF-related materials, further attention should be directed towards solving the problems of high BBB) permeability, avoidance of off-targeting, optimization of targeting strategies, and low immunogenicity.

The BBB, a specialized barrier that restricts many substances from entering the brain, has been a challenge for the effectiveness of certain drugs in treating neurological disorders. To overcome this problem, a Trojan Horse effect has been developed, which targets the BBB. Labeled proteins, such as specific adhesion molecules on the surface of BBB vascular endothelial cells and transferrin receptors, can be incorporated into NPs to achieve high BBB permeability [28,29]. Additionally, short peptides that exhibit good BBB permeability, such as rabies virus glycoprotein [26], BBB transport peptide (TGN peptide) [30], and B6

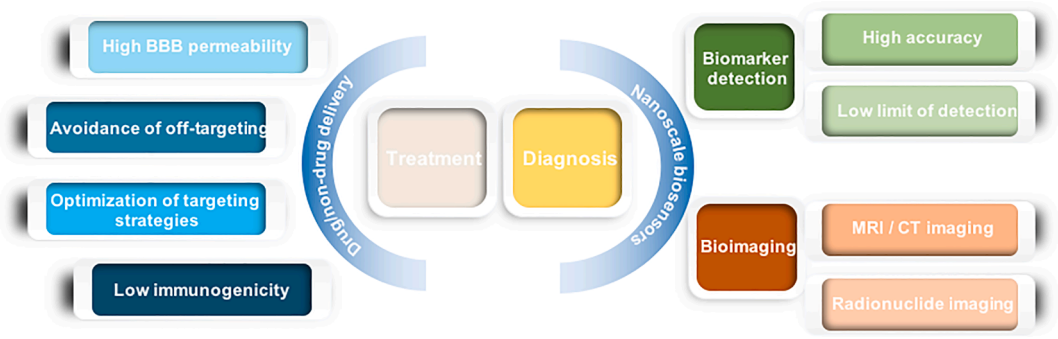

Fig. 1. The potential of MOFs for biomedical applications. Due to the advantages of MOF materials, especially at the nanoscale level, in disease treatment and diagnosis, they have garnered widespread attention in the field of biomedicine [27]. On one hand, the problems of BBB obstruction, off-target effects, poor targeting strategies, and immunogenicity induction have been overcome by MOFs, which are utilized as drug/non-drug delivery systems for disease treatment. On the other hand, with the improvement in accuracy and limit of detection of nanoscale MOF sensors and probes, MOFs can be employed in the detection of biomarkers and biomedical imaging, thereby facilitating early diseases diagnosis.

peptide [31], can be modified on the surface of NPs.

The potential off-target problem of drugs that fail to target diseased tissues, cells, or pathogens represents another significant limitation in the treatment of neurological disorders. The efficacy of a drug depends not only on its own potency but also on its ability to accumulate at the site of the lesion. Therefore, an assessment of both the pharmacokinetic effects of a drug in the systemic system and the concentration of the drug at the site of the lesion, as well as its effect on specific pathogenic molecules, is necessary. Precision nanomedicine is expected to address these challenges by reducing drug accumulation in non-target tissues and increasing the accumulation of drugs at lesion sites. With the rapid development of nanomedicine, nanomaterial-loaded drugs have the potential to reach diseased tissues, penetrate diseased cells, and distribute to subcellular organelles. A study involving the glycoengineering of artificial receptors through metabolic glycoengineering and self-triggered click chemistry demonstrated the successful delivery of N-azidoacetylmannosamine-carrying MOFs to microglia [32]. Dysfunction of mitochondria, a major site of aerobic metabolism, is implicated in the pathological processes of most diseases throughout the body. By employing the lipid insertion method, the mitochondria-targeting ligand triphenylphosphine (TPP) can be effectively localized to mitochondria by inserting TPP onto the surface of NPs [26].

Two well-known pathological features of AD are the extracellular accumulation of Aβ and the hyperphosphorylation of tau protein. Countless attempts have been made by researchers to inhibit the neurotoxicity of Aβ and phosphorylated tau, including the use of nanomedicine for targeted delivery to halt the production and accumulation of both. The targeted removal of pathological Aβ and phosphorylated tau can be achieved through biological strategies. For example, NPs can be attached to targeted short peptides such as LPFFD [33], GGGKLVFF (Aβ targeting peptides) [34], and VQIVYK (tau aggregation motif) [35]. Furthermore, affinity tracers such as thioflavin dyes [32], thioflavin T derivatives (for trapping Aβ aggregates) [36], as well as T807 [37] and MK6240 [38] (for tau tracing), can be attached to the surface of NPs. This allows for selective trapping of Aβ aggregates or phosphorylated tau protein. Intense research has focused on physical strategies, including ROS-dependent photodynamic therapy (PDT) [33,36,39] and local heat-dependent photothermal therapy (PTT) [40], to promote the depolymerization of Aβ protofibrils. PDT, commonly used for ROS generation, produces additional ROS during treatment that have toxic effects on neurons. Therefore, efforts need to be made to control or minimize the generation of these additional ROS to achieve depolymerization of Aβ protofibrils with minimum toxic effects or to explore the use of oxygen-independent photosensitizers before PDT is translated into clinical practice. PTT involves inducing local hyperthermia in response to NIR irradiation, inhibiting the structural conversion of pathological Aβ and preventing aggregation. This therapy also promotes the depolymerization of existing Aβ protofibrils [41]. During PTT treatment, it is crucial to ensure that local hyperthermia causes minimal damage to surrounding tissues and that the damage is reversible.

Strategies such as nanoparticle encapsulation [42] and immune tolerance induction [43] have been proposed by researchers to enhance the biosafety of NPs and prevent the immune response triggered by their presence as foreign entities within the host. Using this idea, it has been shown that biologically modified nanocarriers have been shown to be safe drug delivery systems. Specifically, erythrocytes possess a distinctive biological function that prolongs the retention time of nanosystems in the organism, decreases uptake by the reticuloendothelial system, and mitigates immune recognition, making erythrocyte membrane-encapsulated nanocarriers an ideal vehicle for drug delivery [26]. As therapeutic material-related agents are typically non-clinical species, they can be classified as exogenous and elicit an immune response. Several methods are currently available to induce immune tolerance without compromising the overall function of the immune system [43]. These methods include the utilization of human immunoglobulin G1 (IgG 1) in immunotolerant mice, the intravenous administration of high doses of soluble antigens to establish long-lasting antigen-specific immune tolerance, and the induction of neonatal immune tolerance. Furthermore, it is feasible to incorporate polyethylene glycol (PEG) onto NP surfaces through protein PEGylation [44] or to employ low-toxicity and degradable components like silica [34] or poly(lactic-co-glycolic acid) (PLGA) [31], to coat the NP material, thereby reducing NP toxicity and degradability.

In addition to drug delivery, NPs can also transport non-drug substances, such as gene editing tools. Genetic editing technologies have the capability to target the mutated genes underlying neurological disorders and are anticipated to rectify the dysfunctions caused by these genes. This provides a promising avenue for treating rare and orphan diseases. Effective delivery methods are essential for the successful application of genetic editing technologies in the context of such diseases. Such delivery methods not only overcome the limitations posed by the BBB but also circumvent safety concerns associated with viral vector delivery, thus making NPs-mediated delivery systems a safer alternative [42].

The field of nanomedicine is rapidly evolving with a focus on safety, efficacy, and personalization, which enable the achievement of multi-target and diversified treatment pathways for diseases. Importantly, the utilization of nanomedicine has the potential to revolutionize the development of drugs for challenging diseases. Furthermore, aside from their role in drug and non-drug delivery, some nanomaterials themselves possess protective effects, such as antioxidant and anti-inflammatory properties. For instance, black phosphorus itself exhibits antioxidant effects [36], while manganese porphyrin conjugates in Mn-MOF carriers can imitate the functions of natural superoxide dismutase

(SOD) and catalase (CAT) and are thus involved in the regulation of redox reactions [32]. Additionally, cerium nanocrystals (CeNCs) can inhibit the hyperphosphorylation of tau protein and scavenge ROS [37]. Nanocarriers are not only capable of delivering a single drug but can also simultaneously load multiple drugs, thereby enabling the co-delivery of drugs.

It is known that most clinical diseases have an insidious onset and do not exhibit the dominant features until the endpoint event occurs. Consequently, the medical community has a pressing need for diagnostic tools that can achieve early disease detection, aiming to facilitate early detection, diagnosis, and treatment. In recent years, nanomedicine has made significant advancements, particularly through the application of nanoprobes, which has opened up new possibilities for early disease diagnosis. Nanomedicine can enhance the design of nanoscale sensors and probes, thereby improving accuracy and limit of detection (LOD). These nanoprobes can be conjugated with peptides, antibodies, or other targeting ligands to specifically bind to surface molecules of specific tissues or cells. By utilizing fluorescence (FL), colorimetric, electrochemiluminescence (ECL), fluorescence resonance energy transfer (FRET), and photoelectrochemical cells (PEC), novel biosensors can be created to evaluate specific pathological processes or mechanisms. Furthermore, nanomaterials also have the capability to conduct bioimaging. Nanoscale Fe-containing MOF, as an exceptional nanocarrier, possesses excellent imaging properties [38]. Paramagnetic gadolinium oxide and superparamagnetic iron oxide NPs, functioning as two magnetic resonance contrast agents, can be utilized to label specific cells for cellular-level MRI detection [45]. Radionuclide imaging can also be facilitated by employing longer half-life metal positron nuclides such as Zr and Cu [46].

Nanotechnology, an interdisciplinary field at the forefront of modern science and technology, has allowed the scaling down of MOF materials to the nanoscale and has revolutionized medicine by exploring the molecular world. With the continuous development of nanotechnology and the deepening of pathology research, nanoscale MOFs have made significant progress in the medical field, offering new opportunities for precise and individualized disease diagnosis and treatment.

3. The potential toxicity of MOFs

MOF materials, with their metal clusters and organic linkers, can be designed with precision and allow for different combinations to create hybrid materials with varying components, pore sizes, volumes, and shapes. The modular nature of MOFs allows for seemingly limitless possibilities in their synthesis and design. Additionally, functionalization with organic groups or integration with metal NPs, carbon nanotubes, graphene, and quantum dots can be introduced through post-synthetic modification, allowing for customized functionalities. This has led to MOFs being widely explored in numerous fields [47], including gas separation and storage, catalysis, sensing [48,49], environmental protection such as wastewater treatment and energy conversion and storage [50], as well as biological sensing and imaging, and therapy [51–54] due to their diverse compositions, structures, and adjustable functionalities. However, with the gradual expansion of MOF material applications, concerns regarding their safety have arisen in the scientific community. To proactively address potential risks, scientists have been designing MOFs taking into account the concept of “green chemistry” [55] by using sustainable building blocks and expandable components, selecting mild reaction conditions, using benign solvents, and screening for recyclable catalysts [56]. Despite careful evaluation of the potential contact risks of MOFs and MOF-based composite materials with biology and the environment during the design phase, the safety assessment of MOFs as a whole becomes complex and challenging due to a range of factors such as their composition, synthesis conditions, material stability, and degradability. Furthermore, the balance between efficiency and safety in the production process of MOF materials frequently poses a challenge, hindering their large-scale production.

The human body represents a complex biological system composed of different cells, tissues, and organs. Before the clinical use of MOFs, it is necessary to explore the interaction between MOF materials and different levels (cellular, organ, and systemic) of the human body. Existing research mostly discusses the potential toxicity of MOF materials on individual cell lines or animals based on in vitro, in vivo, or combined in vitro and in vivo assessments. In vivo evaluation of the potential toxicity, biodistribution, and metabolism of MOFs uses animal models, including mammals such as rats [57–60], mice [47,61,62], zebrafish (Dario rerio) [63], amphipods [64] and galleria mellonella [65]. However, due to ethical constraints, zebrafish and amphipods are becoming increasingly popular choices as alternatives to mammals. Overall, this review aims to use these and other works to focus on the use of MOFs used in biological diagnosis and treatment in recent years.

The toxicity of the inorganic and organic components of MOFs represents the primary concern when designing such materials (Fig. 2). The toxicity of MOFs is generally measured in terms of the individual toxicities of these two components. The toxicity of inorganic metals or metal oxides is closely related to the specific type and dose of metal ions and their oxidation states [66]. Previous studies have compared the toxic effects of various metal ions in MOFs, with Ca, Bi, and Eu showing the least toxicity, Ti, Fe, Co, Al, and Cr exhibiting slight toxicity, Zr, Mg, Gd, Ni, and Zn showing moderate toxicity, and Cu or Mn exhibiting the highest metal toxicity [47]. This may be due to the poor stability of some of these MOFs and their high degree of degradation, resulting in the release of a large amount of metal ions into the surrounding medium, thereby seriously disrupting the metabolic processes of organisms, including the disturbance of metal ion homeostasis, interaction with biological molecules such as proteins and peptides, and disruption of redox reactions [57]. Alternatively, the toxicity of organic linkers is linearly related to their hydrophilic/hydrophobic balance, which affects their rate of clearance from the bloodstream [67]. Hydrophilic linkers facilitate the rapid excretion of MOFs in urine, while hydrophobic linkers tend to be excreted more slowly through the liver and spleen.

After entering the body, MOFs undergo pharmacokinetic processes, namely absorption, distribution, metabolism, and excretion (ADME). Different MOFs possess distinct ADME patterns, determined by the varied physicochemical properties of metal ions and organic ligands. These properties include size, aggregation status, surface charge, and shape, as well as chemical and colloid stability. Currently, the physicochemical properties of MOFs serve as the basis for evaluating their toxicity [52]; thus, comprehensive characterization and evaluation of these properties of MOFs is imperative for the future of MOFs in biomedical research.

The toxicity of MOF materials is closely related to particle size, particularly with respect to nanoscale MOFs [52,66]. When MOF particle size is reduced to the nanoscale, the relative surface area increases, making it easy for proteins to adsorb and form protein coronas, severely affecting the dynamics of MOF NPs. Studies have also observed changes in protein corona composition with variations in the exposure environment and duration of MOF NPs, increasing the complexity and unpredictability of their overall toxicity to the body [47]. Furthermore, research has shown that larger NPs (>200 nm) and small NPs (<5–15 nm) pose less harm to the body, as the immune and excretory systems can clear them. However, NPs in the intermediate size range (15–200 nm) are not easily detected by the immune system [47,68], enabling them to pass through physiological barriers and distribute throughout multiple tissues and organs in the circulatory system, disrupting normal physiological functions. Therefore, special attention must be paid to the size of MOF NPs when studying and applying them.

The surface charge of MOFs enhances their ability to adsorb biomolecules such as proteins and lipids. MOF materials with a positively charged surface have a more detrimental effect on cells, as the positively charged species can interact with the negatively charged lipid bilayer of the cell membrane, disrupting the cellular morphology [69]. To reduce the affinity for biomolecules, post-synthetic modification of the MOF

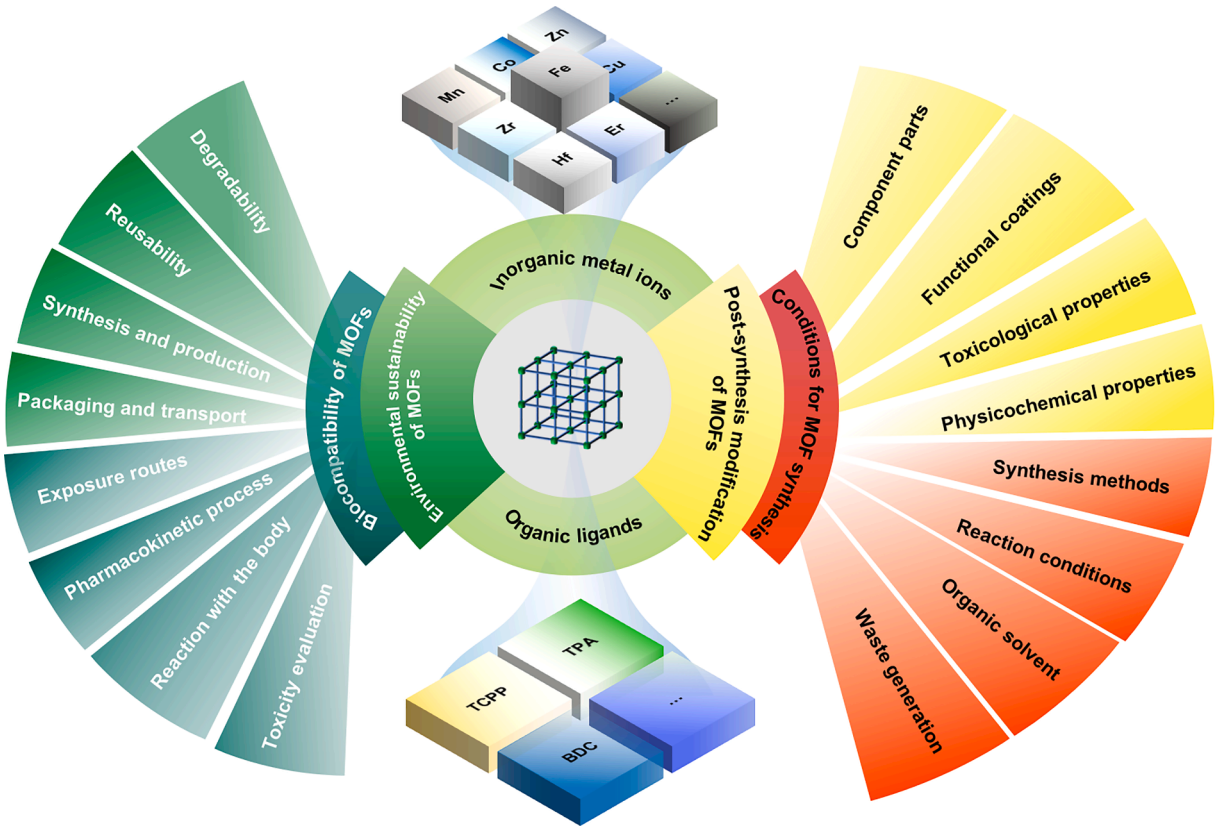

Fig. 2. Potential toxicity of MOFs for biomedical applications. In addition to the core components of inorganic metal ions and organic ligands, MOFs require consideration of synthesis conditions, various aspects of functionalized modifications, biocompatibility and environmental sustainability before being used in biomedical applications, in order to minimize the potential toxicity of the materials.

surface with polymers such as heparin or PEG is often employed [70].

The modification of MOF materials after synthesis can also lead to changes altering their intrinsic properties. These can occur when exposed to various biological environments. Therefore, when evaluating the toxicological properties of MOFs, the route of exposure, such as inhalation, contact with the nasal mucosa or skin, oral ingestion, subcutaneous injection, intramuscular injection, or intravenous injection, needs to be considered. For example, after entering the bloodstream, MOFs first encounter red blood cells, white blood cells, and platelets [47]. Because of this, it is important that the hemolytic activity of MOFs be thoroughly evaluated during intravenous administration. Studies have found that the hemolytic activity of MOFs and their composites is related to particle size, surface properties, and geometric shape [69]. In addition to this effect, upon entering the body as foreign material, MOFs can also cause an immune response. As a semiantigen, MOFs can bind to endogenous proteins and mediate immune stimulation and inflammatory responses [71] which leads to the activation of immune cells and release of cytokines, such as interleukin (IL) −2 and tumor necrosis factor-α. This effect also requires further evaluation in vitro and in vivo. Moreover, the internalization of MOFs in macrophages and peripheral blood mononuclear cells can be tracked by using specific immune fluorescent probes. It has also been shown that MOF NPs can induce procoagulant activity, posing a potential risk of thrombosis [72], and the aggregation of MOF particles can easily lead to embolism [47]. Thus, platelet levels, aggregation, and coagulation parameters, such as thromboelastography, should also be assessed.

Before clinical application, strict, repeated, and comprehensive preclinical studies need to be conducted on MOFs and MOF-based composite materials to establish a standardized toxicity assessment process. The physicochemical properties and biokinetic processes of inorganic metals and organic linkers need to be carefully evaluated, and synthetic conditions must be rigorously controlled with non-toxic solvents. Currently, aqueous-phase or solvent-free synthesis of MOFs is widely regarded as a feasible method [55]. In addition, different cell lines and animal models need to be reasonably selected to evaluate the potential toxicity of MOFs through in vitro and in vivo test systems. The impact of exposure routes and metabolic excretion pathways within the body also needs to be considered. Ultimately, to avoid unnecessary risks, the synthesis, characterization, packaging, and transportation of MOFs need to be carried out under conditions of maximum safety and no pollution.

4. Pathological mechanisms of AD

AD is an age-related neurodegenerative disorder with a complex and diverse pathogenesis. A better understanding of the interplay between AD pathological events and the potential cascading network of resulting reactions can aid in the development of more targeted therapeutic strategies. The two widely accepted core pathological features underlying AD neurodegeneration are the neurotoxicity of Aβ and the hyperphosphorylation of microtubule-associated protein tau. In addition to Aβ and tau pathology, studies have also been performed to investigate the role of microglia and immune cell-mediated neuroimmune-inflammatory axis, brain-gut axis, brain-visceral white adipose tissue (vWAT) axis and other pathological events in the progression of AD. These factors will be the underlying foundation upon which we will seek to describe the etiology of this disease (Fig. 3).

4.1. *Aβ pathology in AD*

Aβ is a 36–43 amino acid peptide generated from the hydrolysis of amyloid precursor protein (APP) by β-secretase (also known as β-site

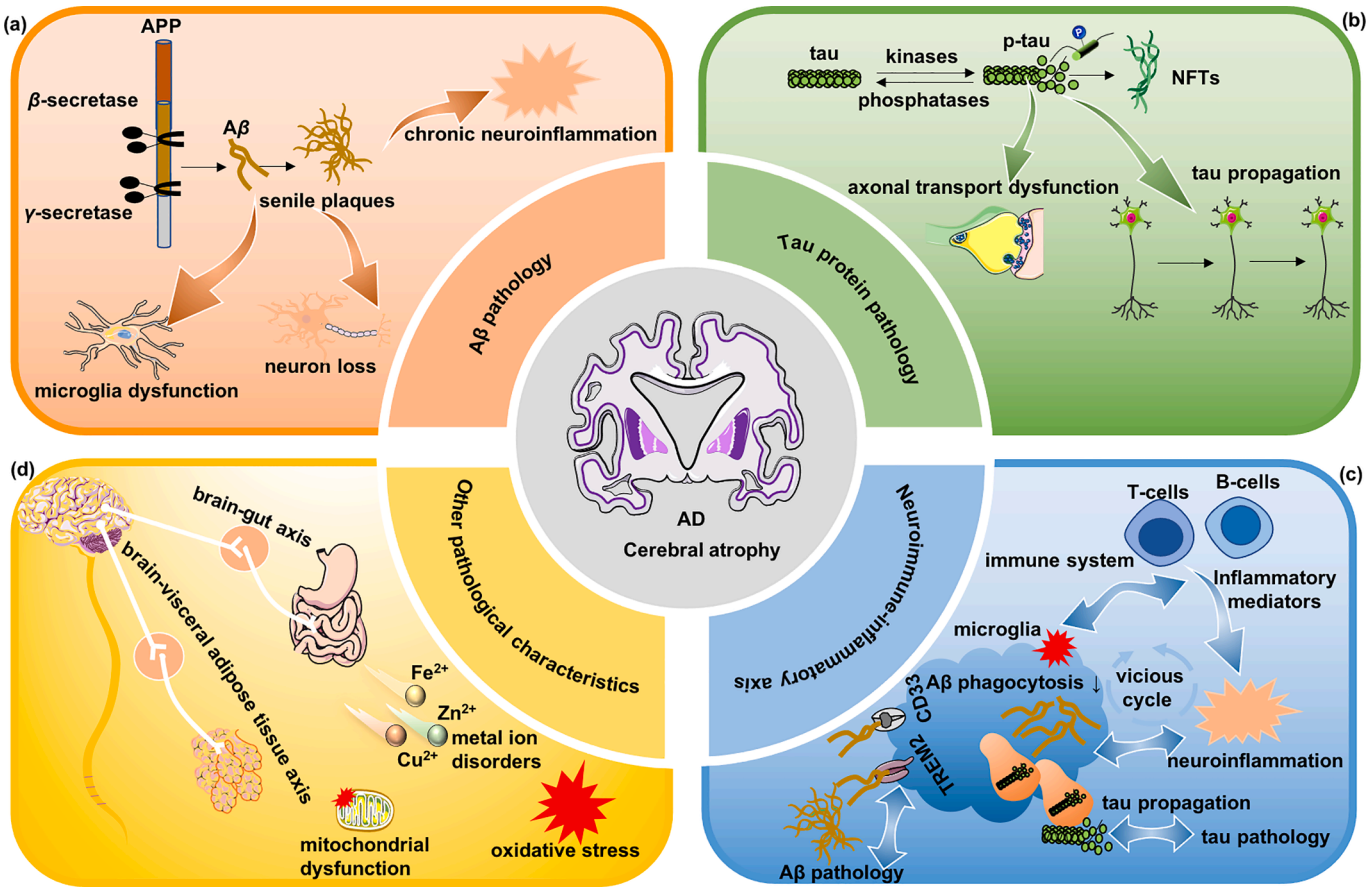

Fig. 3. Pathological mechanisms of AD. **(a)** Aβ pathology in AD. Aβ-mediated neurodegeneration is not only dependent on its own toxicity, but is also associated with other pathological events such as neuronal loss, microglia dysfunction and chronic neuroinflammation; **(b)** Tau protein pathology in AD. Hyperphosphorylated tau proteins lose their physiological function and induce axonal transport dysfunction. Tau ''seeds'' spread between neurons, further amplifying tau protein pathology; **(c)** Neuroimmune-inflammatory axis. Dysfunction of microglia and peripheral adaptive immune T and B lymphocytes mediates neuroinflammation; and **(d)** Other pathological characteristics of AD. The brain-gut axis, the brain-visceral adipose tissue axis and secondary pathological events such as oxidative stress, ion metabolism disorders, mitochondrial dysfunction also mediate AD pathology. No single pathological event exists independently, and multiple pathological events interlock and interact to synergistically contribute to the pathological progression of AD.

APP cleaving enzyme 1, BACE1) and γ-secretase. Among the Aβ peptides, $Aβ_{1-40}$ and $Aβ_{1-42}$ are the most toxic [73,74]. Studies have shown that $Aβ_{42}$ aggregates more rapidly than $Aβ_{40}$ and is the earliest detectable Aβ species in the human brain [74]. Therefore, it is frequently used to induce AD models. Aβ self-assembles into a series of aggregates, including oligomers, protofibrils, and mature fibrils, ultimately forming senile plaques and triggering neuronal toxicity [75]. The mechanism by which Aβ mediates neurotoxicity is complex and depends on the aggregation state, solubility, and distribution location of Aβ. Additionally, the N-terminal modifications of Aβ, such as racemization, isomerization, phosphorylation, and pyroglutamate formation, should not be overlooked for their impact on Aβ neurotoxicity [76–78]. Studies have shown that $Aβ_{N3}$(pE), an N-terminally truncated form of Aβ with pyroglutamate formation at position 3, and pSer8Aβ, a phosphorylated form of Aβ at position 8, increase the concentration of Aβ in the brain, leading to the formation of oligomers and fibrils [73]. These two factors usually indicate different stages of Aβ aggregation, with $Aβ_{N3(pE)}$ appearing in the early stage of Aβ deposition [76], while pSer8Aβ is associated with later plaque formation [78]. As the most common pathogenesis of AD, Aβ-mediated neurodegeneration not only relies on its own toxicity but also triggers downstream events, including (1) tau protein hyperphosphorylation-mediated neuronal toxicity, (2) microglial overactivation and release of inflammatory factors mediating chronic inflammation, (3) Aβ interaction with blood vessels causing cerebral amyloid angiopathy, (4) oxidative stress and mitochondrial dysfunction, and (5) disruptions in metal ion metabolism.

4.2. *Tau protein pathology in AD*

Another core pathological event in AD that has received widespread attention is the hyperphosphorylation of tau protein, which can be excessive and/or abnormal. Tau is a microtubule-associated protein (MAP), encoded by the microtubule-associated protein tau (MAPT) gene located on human chromosome 17 and is involved in controlling cell skeletal integrity [79,80]. Tau comprises four functional domains, including an N-terminal projection domain, a proline-rich region (PRR), the microtubule-binding region (MTBR), and a C-terminal domain. These combine to form six isoforms of tau in the adult human brain, which are generated by selective splicing of exons 2, 3, and 10. The 3R and 4R tau isoforms are composed of three or four microtubule-binding repeat sequences at their C-terminus, respectively [81]. In this state, 3R and 4R tau isoforms are generally present in a one-to-one ratio. An abnormal ratio of the two has been reported to be associated with a class of neurodegenerative diseases called tauopathies [82,83]. 3R tau is mainly present in neuronal inclusion bodies in Pick's disease [84], while 4R tau protein assembles into fibers and is involved in progressive supranuclear palsy [85] and corticobasal degeneration pathology [86]. All six isoforms of tau are involved in the neurofibrillary pathology of AD [87]. Under physiological conditions, tau protein needs to go through dynamic phosphorylation and dephosphorylation processes to

participate in and maintain the steady state of its multiple physiological functions. This phosphorylation modification of tau protein is crucial for establishing cell polarity [88] and also acts as a control switch for tau-microtubule binding and dissociation within neurons. Dephosphorylation with microtubule binding contributes to maintaining microtubule structure stability and optimal axonal transport function, while phosphorylation causes tau to dissociate from microtubules and promotes neuronal mitosis [88,89]. Although phosphorylated tau has an important physiological role, excessive or abnormal phosphorylation of tau can make it a pathological hallmark. Coupled with the fact that tau is a hydrophilic "naturally unfolded" protein with a tendency to self-aggregate into β-sheet structures, its phosphorylated form is more likely to form paired helical filaments and further lead to the formation of NFTs [81,88]. Besides phosphorylation modification, tau protein also undergoes post-translational modifications such as glycosylation, acetylation, and nitration. We note that the catecholamine-derived aldehyde metabolite 3,4-dihydroxyphenylglycolaldehyde (DOPEGAL) covalently modifies the side chains of tau in the noradrenergic locus coeruleus (LC). DOPEGAL directly reacts with a primary amine on the K353 residue of tau, stimulating tau to aggregate into denser fibers [90]. However, tau glycosylation modification may inhibit its self-oligomerization. Tau undergoes post-translational modification by adding N-acetylglucosamine (O-GlcNAc) O-linked to several serine and threonine residues. Increasing tau O-GlcNAc can inhibit the accumulation of tau aggregates [91,92].

4.3. *Aβ and tau protein interactions*

The exact mechanism underlying the connection between Aβ and tau pathology remains a subject of controversy. It is generally believed that tau pathology occurs downstream of Aβ; however, prominent tau pathology still exists in other tauopathy neurodegenerative diseases even in the absence of extracellular Aβ deposits [84–86]. To investigate the relationship between Aβ and tau, researchers injected tau oligomers or brain extracts from human tauopathies into P301S tau mice and wild-type human tau protein transgenic mice (ALZ17) to examine the interaction between Aβ and tau. The experimental results showed that both P301S tau and ALZ17 mice developed neurodegenerative changes mediated by tau pathology in their brains [93,94]. The study also found that Aβ and tau, as pathological "seeds" in AD brain, have different temporal and spatial dependencies. Aβ plaques initially affect the neocortex, followed by the allocortex, and finally the subcortex. The progression of this pathology is correlated with the functional and anatomical coupling of brain regions [95]. In contrast, NFTs evolve in a rigid and progressive pattern, and are classified into six stages according to Braak staging. The first two stages (I and II) represent the prodromal phase of AD in which neuronal fiber changes are mainly localized in the transentorhinal region. The third and fourth stages (III and IV) represent mild cognitive impairment and involve the entorhinal and transentorhinal regions. The fifth and sixth stages (V and VI) represent clinically significant AD, in which the pathology further spreads to the isocortical region [96]. The presence of aggregated Aβ peptides or plaques could induce and enhance the initiation and propagation of tau aggregation in functionally relevant brain areas [81]. Although the anatomical relationship between Aβ plaques and NFTs is not clear, studies indicate that Aβ may directly or indirectly interact with tau proteins, promoting the formation of NFTs.

4.4. *Neuroimmune-inflammatory axis*

Immunodeficiency leads to a decrease in the body's ability to resist pathogenic factors from the external environment and is often accompanied by an inflammatory response. When immunity and inflammation occur together, it leads to what is often termed the neuroimmune-inflammation axis. Microglia, the resident innate immune cells of the central nervous system (CNS), play a crucial role in maintaining the homeostasis of the brain's microenvironment. When microglia sense pathological signals such as infection or injury, they are rapidly activated and transition from a ramified to an amoeboid morphology. In the past, M1 pro-inflammatory or M2 anti-inflammatory phenotypes were thought to represent the extreme activation states of microglia in response to different micro-environmental stimuli [97]. However, with the development of single-cell sequencing and proteomics, a new classification method for microglia has been developed to better reflect their functional states and environmental dependency, such as morphologically activated microglia (PAM), disease-associated microglia (DAM), and microglia neurodegenerative phenotype (MGnD) [7,98,99]. In AD pathology, microglia play a dual role. In the early stage, microglia are activated to phagocytose and clear Aβ, exerting a neuroprotective effect. As the disease progresses, microglia downregulate homeostatic genes and transition to a DAM state [99]. As a result of their over-activated state, the release of large amounts of inflammatory mediators results in chronic inflammation. MGnD represents a neurodegenerative change in microglia mediated by the upregulation of the apolipoprotein E (APOE) gene which is associated with Aβ plaques in the cortical neurons of AD [98]. The inappropriate activation of these microglial cells can lead to a vicious circle of AD neuroinflammation and the chronic inflammatory process. Both are mediated by either the microglial activation or senescent microglia and can be caused by reduced migratory and phagocytic properties (6). Senescent microglia, accompanied by an increase in senescence markers, have been found in the brains of AD patients, especially those with late-onset AD [100,101]. Studies have shown that the continuous proliferation of microglia leads to replicative senescence of themselves and the appearance of DAM, which in turn exacerbates Aβ accumulation and synaptic injuries, leading to AD pathology [100].

Microglia express most of the genes associated with AD risk [97], and interact with Aβ and phosphorylated tau, promoting or inhibiting AD pathology. These genes include: (1) genes that promote Aβ clearance such as scavenger receptors (SR)-A, complement receptor 1 (CR1), and ATP-binding cassette transporter A7 (ABCA7); (2) genes that inhibit Aβ clearance such as APOEε4 and CD33; (3) genes that have a dichotomous role in the Aβ clearance such as CD36, the receptor for advanced glycation end products (RAGE), and triggering the receptor expressed on myeloid cells 2 (TREM2); (4) genes that inhibit tau spreading and phosphorylation such as CX3C chemokine receptor 1 (CX3CR1) and TREM2; and (5) genes that promote tau pathology such as colony-stimulating factor 1 receptor (CSF1R) and APOEε4.

There is growing evidence that adaptive immune cells, specifically T lymphocytes, infiltrate AD brain tissue. The BBB of AD patients is disrupted and dysfunctional, allowing peripheral immune cells to infiltrate the brain tissue (7). Under steady-state conditions, adaptive immune T lymphocytes can maintain the dynamic balance of brain tissue function. However, their precise role in the AD pathogenesis is still not clear, and the mechanisms behind their excessive infiltration and abnormal activation in AD brain tissue are yet to be explored. Several studies have found that the number of $CD4^+$ and $CD8^+$ T cells in the brain parenchyma and cerebrospinal fluid of AD patients is significantly higher than that of the normal control group, with $CD8^+$ T cells being the predominant population [102]. $CD8^+$ T lymphocytes can differentiate into cytotoxic cells, suggesting that infiltrated T cells may have cytotoxicity and be involved in the pathogenesis of AD. Limited observations have shown that the increased infiltration of T cells directly interacts with microglia, promoting the secretion of inflammatory mediators and thus, participating in AD neuroinflammation. Activated microglia can present self-antigens that have engulfed Aβ and phosphorylated tau to $CD4^+$ and $CD8^+$ T cells via MHC I/II molecules [103]. Upregulation of MHC II expression in microglia is associated with neuroinflammation and neurodegeneration. Research has confirmed that microglia activate T-helper cells (Th) expressing eomesodermin by upregulating type I interferon (IFN) and MHC II expression, leading to neurodegeneration [104]. Conversely, aberrantly activated T-cells also affect the functional

state of glial cells. Two important pro-inflammatory T-helper cell subtypes, Th1 and Th17, secrete a series of inflammatory factors targeting activated microglia and astrocytes, promoting Aβ aggregation and neuroinflammation [102,105]. Overall, the aberrant phenotype and functional impairment of T-cells in AD, interacting with Aβ, phosphorylated tau and glial cells, are important factors promoting inflammatory reactions and neuronal loss, ultimately resulting in the worsening of AD pathology. Therefore, disease-modifying therapies targeting different T-cell subtypes may be possible interventions to alter the progression of AD pathology.

Currently, debate surrounds the exact role of B-cells in the neurodegenerative mechanisms of AD. Under antigen stimulation, B-cells can differentiate into plasma cells, secreting immunoglobulins and executing humoral immune functions. The increase of immunoglobulins in AD pathology can enhance Aβ clearance [106]. Limited research has found that in the early stages of AD, B-cell depletion significantly accelerates leading to an increased Aβ burden [54]. However, conflicting research has found a significant increase in the frequency of activated B-cells expressing inflammatory cytokines such as IL-6/10 and IFN-γ in the circulation and secondary lymphoid organs of triple-transgenic AD mice, compared to the control group, with a higher number of B-cells. In contrast, genetically modified mice with functional B-cells showed better cognitive function than the triple-transgenic AD mice [107], further suggesting that pathogenic B-cells may be involved in AD pathology. Together, these studies suggest that therapeutic interventions targeting peripheral immune T and B lymphocytes have the potential to alter the progression of AD pathology. However, to date, the role of peripheral immune cells such as adaptive immune cells (T or B lymphocytes) and innate immune cells (NK cells, monocytes, and dendritic cells) in AD remains poorly understood, requiring further research to provide a more comprehensive theoretical basis.

4.5. Other pathological characteristics of AD

GV-971 is a low molecular weight sodium oligosaccharide that has been approved in China for the treatment of mild to moderate AD [108]. This drug exerts neuroprotective effects through the following mechanisms: reshaping gut microbiota, inhibiting the accumulation of phenylalanine and isoleucine in peripheral blood, and suppressing the differentiation and proliferation of pro-inflammatory Th1 cells, which aids by inhibiting the excessive activation of pro-inflammatory microglia [109]. The advent of GV-971 has sparked a surge in research on the brain-gut axis in recent years. The brain-gut axis transmits information bidirectionally, communicating through neural, immune, endocrine, and metabolic signaling pathways. It is known that the BBB is damaged in AD patients, and gut microbiota and pro-inflammatory factors such as lipopolysaccharides or amyloid proteins released may infiltrate brain tissue through the damaged BBB, exacerbating Aβ neurotoxicity and neuroinflammatory responses [110]. Corresponding to gut microbiota is oral colonizing bacteria, disrupted oral microbiota, and periodontitis. These have also been reported to be involved in AD pathology. As the major pathogenic bacterium in chronic periodontitis, *Porphyromonas gingivalis* has been found in the brains of AD patients [111]. By infecting mice with *Porphyromonas gingivalis*, researchers found that this bacterium and its toxic component, gingipains, were present in their brains alongside toxic peptide $A\beta_{1\text{-}42}$ [112], the production of which can be prevented with the introduction of gingipain inhibitors and has the added benefit of preventing neuroinflammatory responses. In recent years, studies have explored the interactions between the brain and vWAT, a phenomenon referred to as the brain-vWAT axis (BVA). Research has shown that the accumulation of vWAT significantly increases the risk of developing AD in elderly people over the age of 60 [113]. The potential mechanisms underlying the BVA and AD pathology may be related to vWAT metabolites, immune properties, and regulation of insulin resistance [114]. The pathological mechanisms of AD are complex and varied. In addition to the few aspects mentioned above, secondary pathological events such as oxidative stress, ion metabolism disorders, and mitochondrial dysfunction also play an important role in the progression of AD pathology.

5. MOF-enabled diagnosis and treatment of AD

Current clinical treatments for AD are limited, with approved drugs only providing marginal symptom improvement, particularly for those in advanced stages of the disease. As a result, clinicians are forced to intervene aggressively in the early stages of AD to slow disease progression. Therefore, the development of novel biosensors and bioimaging agents is essential for the early diagnosis of AD. Equally important is the exploitation of promising BBB-permeable drugs to stop or reverse the course of the disease. In the following section, we provide a detailed account of MOF-related research concerning the diagnosis and treatment of AD.

5.1. MOFs for AD diagnosis

Given the current state of research on AD, the pressing scientific challenge is to develop assays for key pathological markers that can detect the disease early in its course. MOFs are ideal materials for biosensor construction due to their large specific surface area, tunable pore size, diverse functions, and rich density of active sites. Recent studies have focused on using MOF materials to detect AD pathological markers, with most studies targeting Aβ peptides or oligomers. A few studies have also detected and identified phosphorylated tau proteins, presenilin 1, BACE1, and neurocholinergic transmitters and are shown in Fig. 4 and listed in Table 1.

5.1.1. Aβ-related pathological markers for AD

Current methods for detecting Aβ include the use of antibodies and Apts for specific recognition, as well as metal ions and fluorescent dyes for adsorption. To create simple, inexpensive, and sensitive assays, scientists have combined these with other methods to enhance their efficiency. These include FL, colorimetric, ECL, FRET, and PEC to develop novel biosensors.

Among the various techniques, antibody-based specific recognition is the most commonly used. In 2017, Chen et al. developed a sandwich-type electrochemical immunosensing platform based on Zn-MOF with ferrocene (Fc) as the signal tag, which demonstrated high sensitivity for detecting Aβ [115]. The Fc-Zn-MOF electrochemical signal tag was created by post-synthetic modification of Zn-MOF, with Fc encapsulated within the Zn-MOF. It was then surface-modified with AuNPs (Au@Fc-Zn-MOF) and loaded with the detection of anti-Aβ antibody Ab_2 to construct the Ab_2 bioconjugate (Ab_2/Au@Fc-Zn-MOF). The immunosensor interface was created by coating the surface of a glassy carbon electrode (GCE) with PAMAM-graphene (Gra) to obtain an amino-functionalized sensing interface, and AuNPs/PAMAM-Gra/GCE was obtained by amino-Au affinity. The Aβ concentration was determined from the square wave voltammetric (SWV) response of the immunosensor, where the SWV signal response increased with increasing Aβ concentration. The logarithm of the oxidation peak current versus the target Aβ concentration was linear between 10^{-4} and 100 ng/mL, with a LOD of 0.03 pg/mL and a recovery of 90–110.30 %.

In 2019, Cao and colleagues developed a sandwich ECL-RET (resonance energy transfer) immunosensor with high sensitivity and strong specificity for detecting Aβ (Fig. 5**a**) [116]. The ECL donor platform of this sensor consisted of a g-C_3N_4@Au NPs composite, composed of graphite carbon nitride (g-C_3N_4) and Au NPs, coated on the surface of a GCE, which effectively immobilized Ab_1. Meanwhile, Pd NPs@NH_2-MIL-53 was obtained by an internal reduction method and used as an ECL acceptor labelled on Ab_2. The ECL donor platform exhibited a stronger and more stable cathodic emission light, but the ECL emission spectra of g-C_3N_4 and Pd NPs@NH_2-MIL-53 had a large overlap with the ultraviolet–visible (UV–Vis) absorption spectra of NH_2-MIL-53, resulting

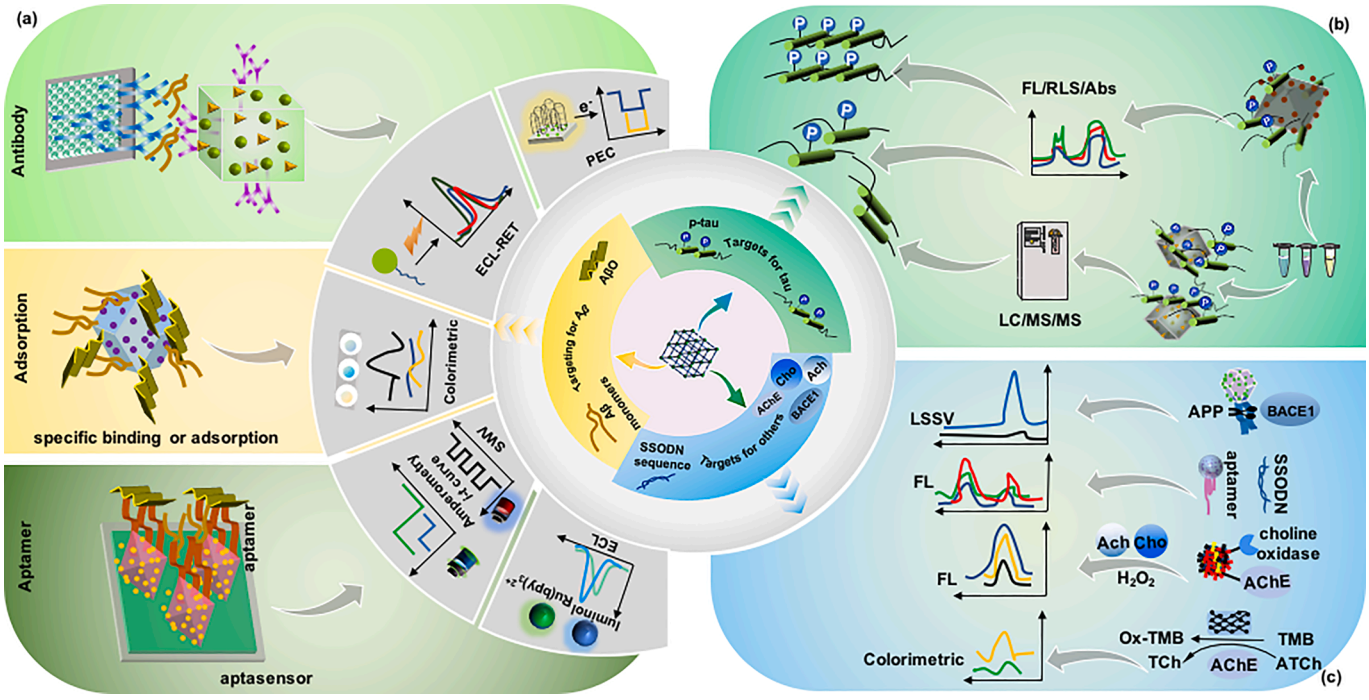

Fig. 4. MOF-based biosensors for detecting AD biomarkers. Current methods for the detection of Aβ pathological markers based on MOFs (**a**) include the use of antibodies and aptamers (Apts) for specific recognition, as well as metal ions and fluorescent dyes for powerful adsorption, which are combined with electrochemistry (SWV, amperometry i-t curve), FL, colorimetric, ECL, FRET and PEC to form novel body fluid biosensors. In addition, MOF-associated biosensors are being used to detect tau-related pathological markers (**b**) by integrating multiple analytical techniques, including LC/MS/MS, Abs, FL and RLS, to accurately detect and distinguish the presence or absence of phosphorylated proteins and their patterning. Likewise, the detection of other pathological markers of AD (**c**) includes using MOF-associated biosensors combined with LSSV, FL, and colorimetric methods, including BACE1, SSODN sequence, AChE, Cho, and Ach.

in attenuation of the ECL signal. However, the apparent quenching effect of ECL-RET between the donor platform and the acceptor of the ECL immunosensor successfully achieved ultra-sensitive Aβ detection. The sensor has a linear concentration detection range of 10^{-5}–50 ng/mL, and a LOD of 3.4 fg/mL, and a recovery of 95–105 %. In the same year, Cao's team also developed a dual-signal sandwich electrochemical immunosensor based on SWV and amperometry *i-t* curve methods for detecting Aβ concentrations (Fig. 5**b**) [117]. The sandwich sensor comprises a matrix material at the bottom, a signal tag at the top, and the target Aβ in between. Cu-Al_2O_3-g-C_3N_4 was synthesized by hydrothermal method using g-C_3N_4, $Al(NO_3)_3{\cdot}9H_2O$, and $Cu(NO_3)_2{\cdot}3H_2O$. Subsequently, Cu-Al_2O_3-g-C_3N_4 and Na_2PdCl_4 were used to synthesize Cu-Al_2O_3-g-C_3N_4-Pd through ultrasonic and internal reduction methods, with Cu-Al_2O_3-g-C_3N_4-Pd serving as the matrix material providing the crucial electrochemical signal for the immunosensor. Cu-Al_2O_3-g-C_3N_4-Pd was then coated onto a GCE and Pd NPs were used to immobilize Ab_1 through the Pd-NH_2 bond. The amperometry *i-t* curve method was employed to detect the current signal of Cu-Al_2O_3-g-C_3N_4-Pd catalyzed reduction of H_2O_2. The current signal decreased as Aβ concentration increased, and a linear relationship was observed between Aβ and the current signal in the concentration range of 10^{-5}–100 ng/mL. The method yielded recoveries of 98.66–102.96 %. Similarly, UiO-66 was also examined for its sensing effectiveness [117]. Polyaniline (PANI) was used to modify UiO-66 to improve its electrical conductivity and adsorption capacity and to immobilize Ab_2 via amino groups. Methylene blue (MB) was used as a signaling marker to label Ab_2. These components formed UiO-66@PANI-MB/Ab_2, which was incubated on the surface of the GCE electrode. The SWV method was used to detect the electrochemical reaction signal of UiO-66@PANI-MB in PBS solution with Aβ. The SWV electrochemical signal was enhanced with increasing Aβ concentration, and a linear correlation was observed between the two with a LOD of 3.3 fg/mL, corresponding to a recovery of 98.88–103.10 %.

To date, various strategies have been explored for biomolecule detection using ECL technology, including immunosensors and aptasensors. Luminol and tris(2,2′-bipyridyl)-ruthenium (II) [$Ru(bpy)_3^{2+}$] are commonly used ECL luminophores. Wei's group reported a sandwich-type ECL immunosensor for Aβ detection based on antigen–antibody immunoreactivity, using $Ru(bpy)_3^{2+}$ as the ECL luminol [118]. The ECL luminescence donors were $Ru(bpy)_3^{2+}$/zinc oxalate MOFs, and the acceptors were Au@NiFe MOFs and, when combined, demonstrated a significant improvement in sensitivity for Aβ detection due to the double quenching effect of ECL fluorescence. The ECL emission spectra of $Ru(bpy)_3^{2+}$ overlapped with the UV–Vis absorption spectra of both NiFe-based MOFs and Au@NiFe MOFs, allowing for double quenching of $Ru(bpy)_3^{2+}$ fluorescence between the luminescence donor and acceptor through RET. The luminescent donor and acceptor bound to Ab_1 and Ab_2, respectively, achieved ultra-sensitive Aβ detection through specific binding to Aβ. The ECL response of this immunosensor was linear in the logarithm of the Aβ concentration in the range of 10^{-4}–50 ng/mL, with a LOD of 13.8 fg/mL. The recovery of artificial CSF Aβ detection was 99–100.76 %.

A similar sandwich-type ECL immunosensor based on NH_2-UiO-66 and MIL-101 dual MOFs was developed by Cao's team in 2020, also using $Ru(bpy)_3^{2+}$-based ECL luminophores (Fig. 5**c**) [119]. The sensor used water-soluble $Ru(bpy)_3^{2+}$ encapsulated by NH_2-UiO-66 ($Ru(bpy)_3^{2+}$/ NH_2-UiO-66) to ensure the stability of its luminol against external interference. Meanwhile, MoS_2 quantum dots (MoS_2 QDs) act as $Ru(bpy)_3^{2+}$ quenchers. The macromolecule MIL-101 was also found to reduce the ECL signal by blocking electron transfer. $Ru(bpy)_3^{2+}$/ NH_2-UiO-66 was added dropwise to the surface of the GCE electrode which then coupled to Ab_1, while MIL-101@Au-MoS_2 loaded with Au NPs labelled Ab_2, thus constructing an ECL immunosensor containing a dual-MOF structure that specifically recognizes Aβ. The ECL signal was linear in the logarithm of the Aβ concentration in the range 10^{-5}–50 ng/mL with a LOD of 3.32 fg/mL. The recovery of the assay platform was

Table 1
MOF-associated materials for the detection of AD biomarkers.

Material	Biomarker	Detection media	Assay	Linear range	LOD	Recovery (%)
Au@Fc-Zn-MOF [115]	Aβ	human serum	SWV	10^{-4}–100 ng/mL	0.03 pg/mL	90.00–110.30
Pd NPs@NH_2-MIL-53 [116]	Aβ	human serum	ECL-RET	10^{-5}–50 ng/mL	3.4 fg/mL	95.00–105.00
UiO-66@PANI-MB [117]	Aβ	human serum	SWV, Amperometry *i-t* curve	10^{-5}–100 ng/mL	3.3 fg/mL	98.88–103.10 (SWV), 98.66–102.96 (Amperometry *i-t* curve)
Au@NiFe MOFs, $Ru(bpy)_3^{2+}$/zinc oxalate MOFs [118]	Aβ	artificial CSF	ECL	10^{-4}–50 ng/mL	13.8 fg/mL	99.00–100.76
NH2-UiO-66, MIL-101 [119]	Aβ	artificial CSF, human serum	ECL	10^{-5}–50 ng/mL	3.32 fg/mL	96.34–101.31 (artificial CSF), 96.97–101.92 (human serum)
Bi-MOF [120]	$Aβ_{42}$, $Aβ_{40}$	artificial CSF	PEC	10.0–10^9 fg/mL ($Aβ_{42}$), 1.0–10^6 pg/mL ($Aβ_{40}$)	4.5 fg/mL ($Aβ_{42}$), 0.52 pg/mL ($Aβ_{40}$)	95.40–102.40
L-MOFs [121]	AβO	human serum	FL	0.001–100 ng/mL	0.4 pg/mL	90.00–102.00
AuNPs/Fe-MIL-88NH_2 [122]	AβO	human serum	ECL	0.1–10 pM	71 fM	98.90–105.40
HRP@Fe-MOF [123]	AβO	human serum	UV–Vis spectrophotometry	10^{-4}–10 nM	0.03 pM	90.00–101.00
Ru@MOFs [124]	Aβ	human serum	ECL-RET	10^{-5}–500 ng/mL	3.9 fg/mL	99.20–103.00
Ru@MIL-101(Al) [125]	AβO	human serum	FL	1.0–10^4 pM	0.3 pM	93.01–102.20
AuNPs@CuMOF [126]	AβO	artificial CSF	DPV	0.5–500 fM	0.25 fM	96.00–110.00
CeONP-Res-PCM@ZIF-8/PDA/Apt [127]	AβO	–	FL	10—10^4 nM	3.2 nM	–
ZnCo-ZIF [128]	$Aβ_{40}$	rat CSF	Colorimetric	5–150 nM	1.58 nM	92.52–107.60
H-UCNPs-SiO2@ZIF-8/ BHQ-1 [129]	AβO	–	FL	10^{-4}–10 μM	28.4 pM	–
ThT@Er-MOF [130]	presenilin1 (SSODN), Aβ, Ach	CSF	FL	0–33 nM (SSODN), 0–40 nM (Aβ), 0–8 nM (Ach)	0.517 pM (SSODN), 0.142 nM (Aβ), 0.03226 nM (Ach)	–
ph-AgNPs@MOF [131]	BACE1	human serum	Voltammetric	1–200 pM	0.8 pM	94.90–107.00
2D Hf-BTB nanosheets [132]	tau	mouse cortex	LC/MS/MS	–	–	–
Zr-FeTCPP-MOF [133]	tau	–	3D spectral array:Abs + FL + RSL	–	–	–
TMBDA-MIL-100(Fe) [134]	Cho, Ach	milk (Cho), human serum (Ach)	FL	0.5–10 μM (Cho), 0.1–20 μM (Ach)	0.027 μM (Cho), 0.036 μM (Ach)	100.00 (Cho), 97.00–103.00 (Ach)
Cu-CAT NSs [135]	AChE	human serum	Colorimetric	0.01–4.0 mU/mL	0.01 mU/mL	93.00–101.00
Zn-TCPP(Fe) NSs [136]	AChE	human serum	Colorimetric	0.54–3.93 mU/mL	0.029 mU/mL	96.99–101.10

96.34–101.31 % in artificial cerebrospinal fluid and 96.97–101.92 % in human serum.

An innovative i-motif structure-based switchable PEC immunosensor with a single pH-variable interface and simultaneous detection of $Aβ_{42}$ and $Aβ_{40}$ was reported by the Song WB group in 2022 (Fig. 5**d**) [120]. The PEC sensor was shown to modulate the formation or dissociation of the i-motif structure based on pH which in turn modulates the distance between Au NPs and Bi-MOF (i.e. Bi-TBAPy) to generate separate photocurrents for $Aβ_{42}$ and $Aβ_{40}$, respectively. The Aβ antigen–antibody immunoreaction as well as the lysis and enzyme-catalyzed reactions are used to generate acidic or basic lysates with different corresponding pH values. In the presence of $Aβ_{42}$, the acidic lysate drives the formation of i-motif structures that label Au NPs on thiolated DNA (SH-DNA), enhancing the Bi-TBAPy-mediated cathodic photocurrent density. Alternatively, in the presence of $Aβ_{40}$, the alkaline lysate induces the unravelling of the i-motif structure, pushing the Au NPs-labelled SH-DNA away from the electrode surface and reducing the photocurrent density. The linear concentration ranges for $Aβ_{42}$ and $Aβ_{40}$ detection in this study were 10 fg/mL μg/mL and 1 pg/mL μg/mL, with LODs of 4.5 fg/mL and 0.52 pg/mL, respectively. The recoveries for this PEC sensor were 95.40–102.40 %.

While innovative, the high cost and time-consuming nature of antibody detection has limited their utility. In recent years, Apt has emerged as a promising alternative to antibodies for specific molecular recognition in biosensing. Apt is small, in vitro screened, single-stranded RNA or DNA biorecognition of elements that are easy to synthesize, inexpensive, fast-reacting, and non-immunogenic. They bind specifically to a corresponding ligand to form an aptasensor. Apt has been introduced into biosensing in two main areas. One main interest focuses on developing label-free detection methods for Apt. For example, amino-functionalized Apts and carboxyl-functionalized Fe_3O_4 are conjugated to capture Aβ oligomers (AβO) (Fig. 6**a**) [121]. Anti-DNA antibodies are armored with lanthanide MOFs (L-MOFs) to form luminescent nanocrystals through ultrasonic synthesis, and act as signal tags. The L-MOFs armor the anti-DNA antibodies in a biomimetic mineralization-like manner, protecting them from the external environment while also maintaining their thermal stability under high temperatures. The capture probe Apt-Fe_3O_4 NPs form a fluorescent aptasensor with the signal tag L-MOF. The strong fluorescence intensity of L-MOF is switched off due to light-induced electron transfer from the excited state to the d-shell of unfilled Fe cations on the NP surface. AβO has a higher affinity for Apt containing AβO sequences, and once AβO is detected in blood, the signal tag is released into solution, exciting the strong fluorescence of the aptasensor. This AβO detection platform has the added benefit of

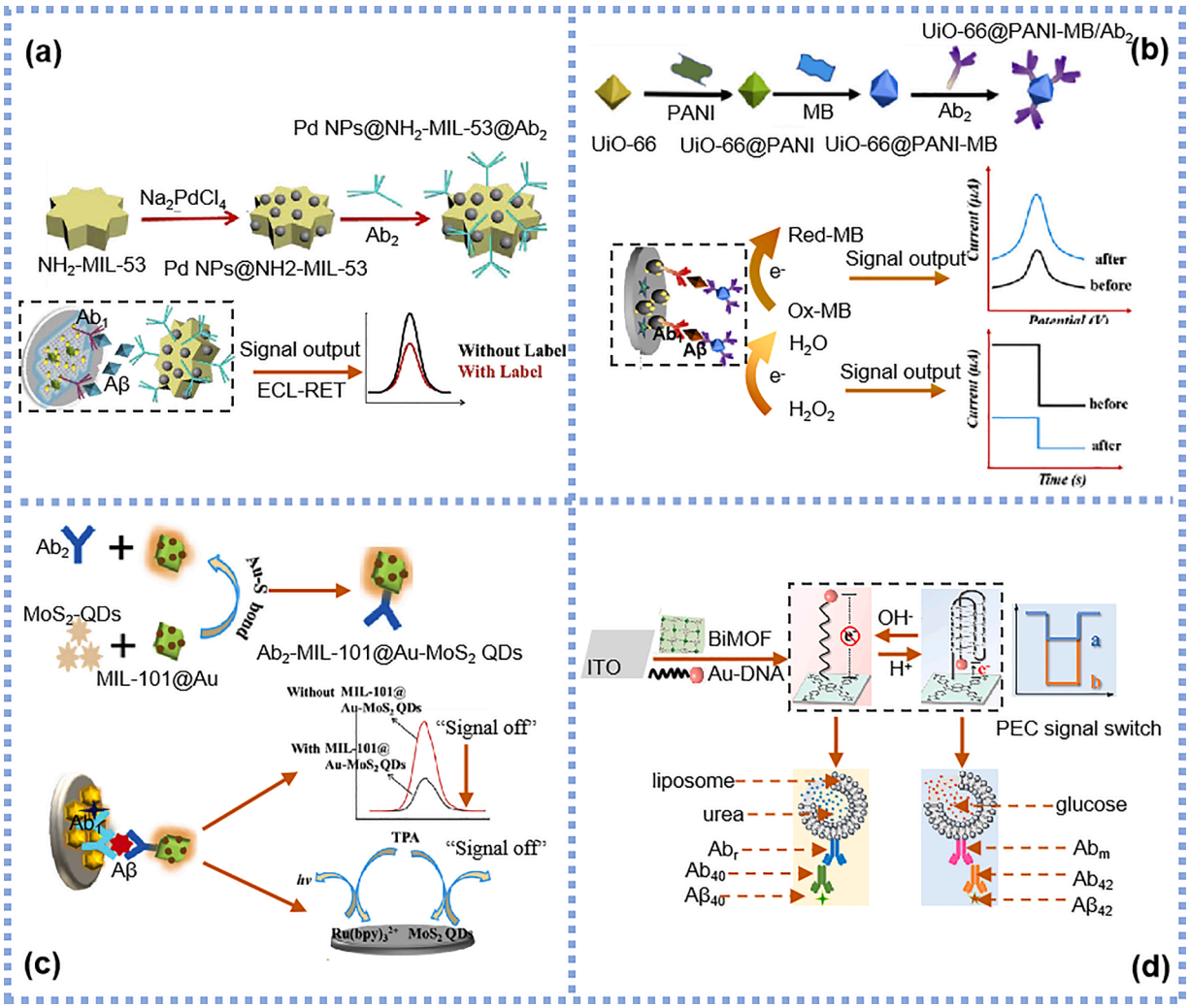

Fig. 5. MOF-based biosensors for detection of Aβ pathology markers by antibody-specific recognition. **(a)** An ultrasensitive sandwich ECL-RET immunosensor for Aβ detection. Reproduced with permission [116]. Copyright 2019 Elsevier B.V. **(b)** A dual-signal sandwich electrochemical immunosensor based on SWV and amperometry *i-t* curve methods for Aβ detection. Reproduced with permission [117]. Copyright 2019 Elsevier B.V. **(c)** A similar sandwich-type ECL immunosensor based on NH_2-UiO-66 and MIL-101 dual MOFs for Aβ detection. Reproduced with permission [119]. Copyright 2019 Elsevier B.V. **(d)** An i-motif structure-based switchable PEC immunosensor with a single pH-variable interface and simultaneous detection of $Aβ_{42}$ and $Aβ_{40}$. Reproduced with permission [120]. Copyright 2022 American Chemical Society.

being reusable, allowing the aptasensor to be recycled by regulating the temperature and has been shown to be reusable at least 10 times while maintaining high aptasensor activity. The label-free Apt assay platform has high sensitivity and specificity for the detection of human serum AβO, with a LOD of 0.4 pg/mL and a linearity range of 0.001–100 ng/mL, enabling the detection of AβO over a wide range of concentrations [121].

Another label-free aptasensor for the detection of AβO was developed by Tu's team in 2021 [122]. The detection platform consists of a substrate electrode with an aptasensor on the surface. Indium-tin oxide (ITO)-coated glass is coated with 3-aminopropyltrimethoxysilane (APTMS) to form a layer of silicone rubber, to which Au NPs/Fe-MIL-88NH_2 are immobilized via Au-N bonding, forming the substrate electrode. The Au-N bond modified AuNPs can effectively improve the ECL capability of luminol. Specific Apt containing AβO DNA sequences are then tightly bound to the AuNPs via Au-S bonds. The aptasensor is based on an ECL method using luminol as a luminescent probe to detect AβO concentrations in peripheral serum. The results of this study showed that the inhibition of the ECL signal of this aptasensor regressed linearly with the logarithm of the AβO concentration, with a linear range of 0.1–10 pM and a LOD of 71 fM.

In order to overcome the low efficacy and weak thermal stability of the biosensor, Fe-MOF armored with horseradish peroxidase (HRP) forms a biomimetic mineralized HRP@Fe-MOF, which has peroxidase activity and catalyzes the color development of 3,3′,5,5′-tetramethylbenzidine (TMB) / H_2O_2. On the other hand, Fe-MOF, due to its Fe (II) ion content, can be oxidized to Fe(III) by H_2O_2 via the Fenton reaction, facilitating the color development reaction. Thus, HRP@Fe-MOF is a signal tag with a dual catalytic effect [123]. AβO Apt is attached to the surface of Fe_3O_4 NPs by carbodiimide cross-linking and then conjugated to the HRP@Fe-MOF signal probe to form an optical biosensor based on UV–Vis spectrophotometry for the detection of AβO. The aptasensor detects AβO in the linear concentration range of 0.0001–10 nM, with an LOD of 0.03 pM and a recovery of 90.00–101.00 %.

The other main area of interest in Apt sensing utilizes a biosensing assay based on aptasensor labelling. The ECL-RET system constructed with luminol $Ru(bpy)_3^{2+}$ functionalized MOF was first reported by Jia's team in 2019 which successfully achieved efficient and sensitive detection of human serum Aβ levels (Fig. 6**b**) [124]. The ECL-RET system is a sandwich-type aptasensor with the first sensing layer comprised of a g-C_3N_4 nanosheet (NS) luminescent donor with an Aβ target in the center. The second sensing layer consists of an ECL-RET receptor with a

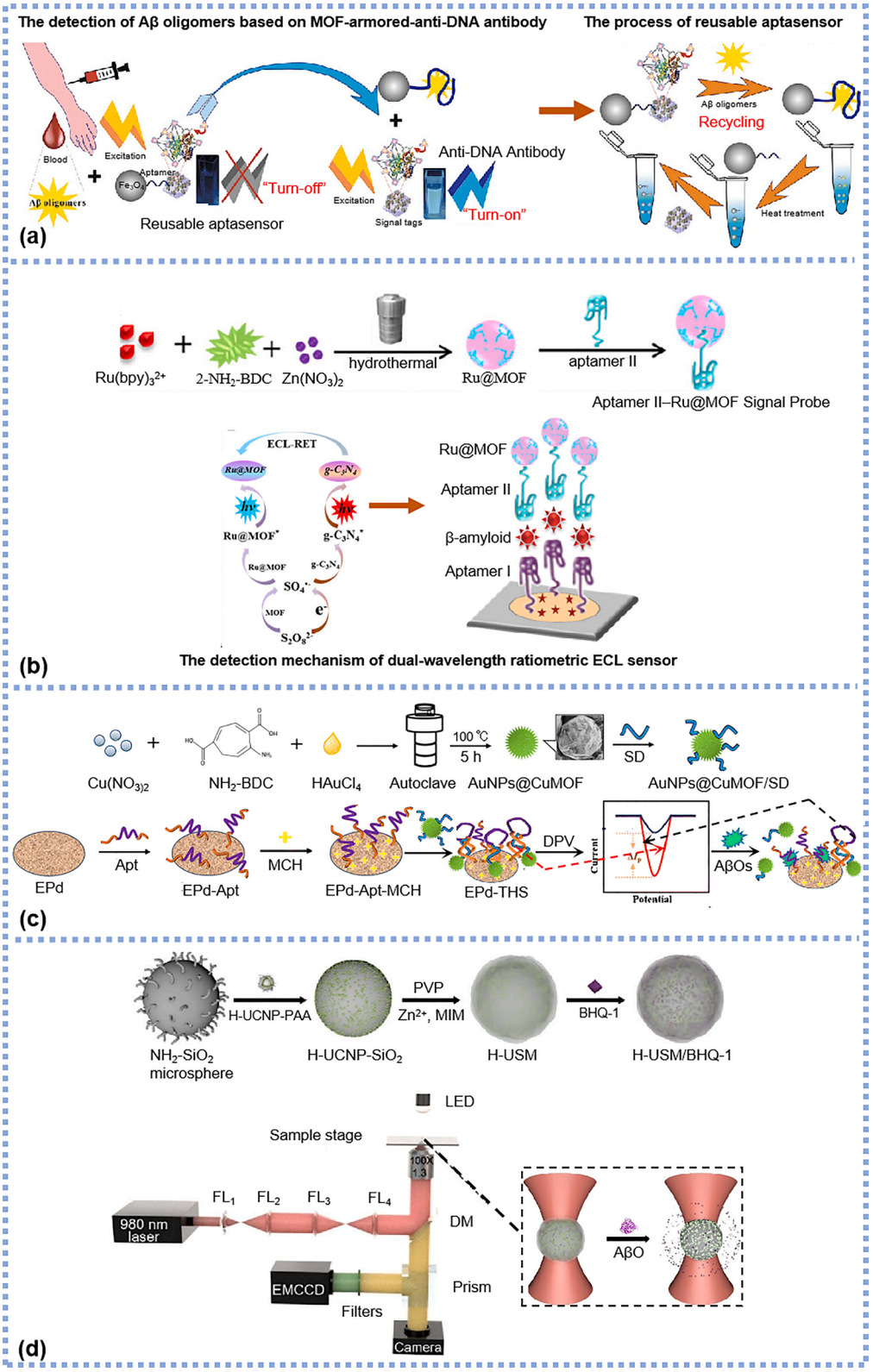

Fig. 6. MOF-based biosensors for detection of Aβ pathology markers by Apt-specific recognition or high-affinity metal ions. **(a)** A label-free, reusable aptasensor for the detection of Aβ oligomers based on MOF-armored-anti-DNA antibody. Reproduced with permission [121]. Copyright Springer-Verlag GmbH Austria, part of Springer Nature 2020. **(b)** An ECL-RET assay system consisting of a luminol $Ru(bpy)_3^{2+}$ functionalized MOF for the efficient and sensitive detection of human serum Aβ. Reproduced with permission [124]. Copyright 2019 American Chemical Society. **(c)** An electrochemical aptasensor based on Apt-labelled Cu-MOF material for the specific detection of AβOs. Reproduced with permission [126]. Copyright The Author(s). **(d)** ZIF-8 encapsulated with lanthanide-doped Ln-UCNPs were used to form fluorescent biosensors for the specific detection of AβO based on the competitive binding of Zn^{2+} to the amino acid of AβO. Reproduced with permission [129]. Copyright 2021 American Chemical Society.

$Ru(bpy)_3^{2+}$-doped MOF (Ru@MOF) linked to an Aβ-Apt II complex. This ECL aptasensor detects Aβ targets based on the principle of dual wavelength ratios. The addition of an Aβ target attenuates the ECL signal of g-C_3N_4 NS (−1.5 V) and enhances the ECL signal response of Ru@MOF (1.1 V). The ECL aptasensor has a linear concentration detection range of 10^{-5}–500 ng/mL, a LOD of 3.9 fg/mL, and a recovery of 99.2–103 %.

To develop a homogeneous and sensitive "turn-on" fluorescence amplification strategy, Zhang's team combined luminescent MOF materials with exonuclease-assisted target recovery [125]. In doing so, they successfully developed a homogeneous "turn-on" fluorometric aptasensor for FRET-based detection of AβOs. The luminescent Ru@MIL-101 (Al) acts as a fluorescent donor with an acceptor consisting of Apt-modified Au NPs to form the tracking agent (Apt-Au NPs/Ru, Al MOF). When AβOs are present in the test sample, the Apt-Au NPs in the tracking agent preferentially bind to the AβOs, causing Ru@MIL-101(Al) to be released and the strong fluorescence signal to be turned on again. The REC JF exonuclease mediates the recovery of the Apt-AβOs complex, leading to an expanded fluorescence signal. AβOs concentrations were detected using a fluorescence spectrophotometer at a fluorescence emission wavelength of 610 nm. The linear concentration range for AβOs detection was found to be 1.0–10^4 pM with a LOD of 0.3 pM. The recovery of this fluorescent aptasensor was 93.01–102.20 %.

To generate an amplifiable and distinguishable electrochemical signal, Jiang's team designed an electrochemical aptasensor based on Cu-MOF material labelled with Apt for the specific detection of AβOs (Fig. 6**c**) [126]. To amplify the electrical signal of the sensor while avoiding the weakening of Apt activity, they used a triple helix switches (THS) coupled to the above Apt-labelled Cu-MOF system to produce electrochemical aptasensor with a switchable mode. The aptasensor is a sandwich-type detection platform. The upper part comprises a signaling displaced-probe (SD) labelled with AuNPs@Cu-MOF. AuNPs@Cu-MOF is synthesized by adding $HAuCl_4$ during the preparation of Cu-MOF, and the SD is attached to its surface to form AuNPs@Cu-MOF/SD. The lower part comprises an electrodeposited palladium electrode (EPd)-Apt-6-mercaptohexanol (MCH) hybridization system with THS. EPd-Apt-MCH is hybridized with AuNPs@Cu-MOF/SD in a buffer containing THS to form EPd-THS. Upon encountering the AβOs target, AβOs-Apt binding triggers DNA displacement, resulting in the release of AuNPs@Cu-MOF/SD from THS. The detection of trace amounts of AβO was successfully achieved by monitoring changes in the differential pulse voltammetry (DPV) response. The linear concentration detection range of this aptasensor was 0.5–500 fM with a LOD of 0.25 fM and a recovery of 96–110 %.

ZIF-8 which is a microporous material has also been used for fluorescence sensing of Apt due to its fluorescence quenching properties [137]. Polydopamine (PDA) is a good photothermal agent with strong absorption of near-infrared (NIR) light; it has a high affinity for the single-stranded DNA conformation of Apt and can exert a high fluorescence quenching effect via fluorescent RET. Due to the presence of functional groups such as catechols and amines on the surface of PDA, it is used as a bioadhesive cross-linking agent to tether ZIF-8 nanocrystals. After ZIF-8 is coated with PDA, Texas Red-labelled AβO Apt is attached to the ZIF-8/PDA nanocomposite via π-π stacking, forming a ZIF-8/PDA/Apt fluorescent aptasensor [127]. The aptasensor shows a high fluorescence signal in the presence of AβO. In contrast, it showed a lower fluorescence signal due to fluorescence quenching caused by the binding of PDA to Apt. Based on this, the sensor showed a specific affinity for AβO and high detection sensitivity, with a good linear relationship between AβO and fluorescence response at 10 nM and 10 μM with an LOD of 3.2 nM.

Metal ions such as Zn^{2+} and Co^{3+} [128], as well as the fluorescent dye thioflavine (ThT) [138], have a high affinity for Aβ leading to the development of biosensors for Aβ detection. In 2021, Li's group developed a fast and sensitive colorimetric biosensor for the quantification of $Aβ_{40}$ monomers, dynamic tracking of the Aβ aggregation process, and screening for Aβ inhibitors [128]. The biosensor is based on the rapid oxidation of a ZnCo zeolitic imidazolate framework (ZnCo-ZIF) to prepare a novel porous bimetallic transition metal oxide nanocage (ZnO-Co_3O_4 NC). The ZnO-Co_3O_4 NCs have peroxidase-like activity, and the bimetallic Zn^{2+} and Co^{3+} in them have a high binding and adsorption capacity to the Aβ monomer. The inhibition of the peroxidase activity of ZnO-Co_3O_4 NCs by different Aβ species (Aβ monomers, oligomers, and protofibrils) varies. This biosensor provides a cheap and simple method for high-throughput detection of Aβ. The colorimetric biosensor operates by oxidizing 3,3′,5,5′-tetramethylbenzidine (TMB) with ZnO-Co_3O_4 NCs, resulting in a change from colorless to blue. However, the presence of $Aβ_{40}$ monomer significantly inhibits the peroxidase activity of ZnO-Co_3O_4 NCs, leading to a more pronounced blue shift. The biosensor successfully detected $Aβ_{40}$ monomer in rat cerebrospinal fluid (CSF), at an absorbance of 652 nm exhibiting linearity with $Aβ_{40}$ concentration in the range of 5–150 nM. The LOD for $Aβ_{40}$ monomer in CSF was 1.58 nM, and the colorimetric recovery was 92.52 %-107.6 %. Similarly, ZIF-8 encapsulated with lanthanide-doped upconversion NPs (Ln-UCNPs) were used to form fluorescent biosensors for the specific detection of AβO based on the competitive binding of Zn^{2+} to the amino acid of AβO (Fig. 6**d**) [129]. To overcome the disadvantages of poor photostability and weak signal-to-noise ratio of fluorescent probes, Tang's team chose Ln-UCNPs with strong upconversion luminescence (UCL) and excellent power dependence as fluorescent probes. The oleic acid (OA)-covered highly doped UCNPs were modified with poly(acrylic acid) (PAA) and attached to the SiO_2 surface, then wrapped with ZIF-8 to form H-UCNPs-SiO_2 (H-USM) microspheres, and finally the black hole quencher molecules BHQ-1 were added to form the final product H-USM/ BHQ-1. The H-USM/ BHQ-1 microspheres, combined with the optical trapping method, amplify the AβO detection signal and detection sensitivity. The quenching molecule BHQ-1 has excellent quenching efficiency for UCL_{540} emission. In the presence of AβO, Zn^{2+} binds to the AβO amino acid, leading to the degradation of ZIF-8 and the release of BHQ-1, with the consequent 'switching on' of the UCL_{540} signal. UCL_{654} was used as the background signal and the UCL_{540}/UCL_{654} ratio as the detection signal. A linear relationship was found between the logarithm of the AβOs concentration from 100 pM to 10 μM and the UCL_{540}/UCL_{654} ratio, with an LOD of 28.4 pM for the fluorescent biosensor.

Another metal ion containing MOF was synthesized by Ding and Wang. 3D $[Er(L)(DMF)_{1.27}]_n$ (Er-MOF) displayed 1D nanopore channels and incorporated terphenyl-3,4″,5-tricarboxylic acid (H_3L) which contains chromophores in the terphenyl moiety [130]. The MOF-based post-synthetic modification encapsulated the cationic fluorescent dye ThT in Er-MOF (ThT@Er-MOF), resulting in a highly sensitive and specifically selective fluorescent sensor for Aβ. The fluorescence intensity exhibited excellent linearity with Aβ concentrations in the range of 0–40 nM, with a LOD of 0.142 nM.

The production of Aβ is closely linked to the activity of the BACE1 enzyme. To detect BACE1 activity, Bi et al. developed an electrochemical assay based on tyrosine-conjugation and AgNPs/Zr-MOF electrochemical labelling [131]. The electrochemical sensor comprises a microwell plate reactor and a screen-printed graphene electrode (SPGE) detector. The tyrosine-containing APP fragment is immobilized on the aminated microplate reactor, while the cytosine-rich AgNPs/Zr-MOF is modified with 4-mercatophenol to form a ph-AgNPs@MOF electrochemical label. This label is cross-linked to the phenolic group of the APP tyrosine via its own phenolic ring. When BACE1 is present in the test sample, the APP peptide is cleaved, leading to the transfer of ph-AgNPs@MOF to the SPGE detector. The electrochemical signal of the AgNPs is detected using linear sweep stripping voltammetry (LSSV). The LSSV peak current is linearly related to the BACE1 concentration in the range of 1–200 pM, with a LOD of 0.8 pM and recoveries in the range of 94.90–107.00 %. This electrochemical sensor was shown to not only quantify the level of human serum BACE1, but could be used to screen for BACE1 inhibitors.

5.1.2. Tau-related pathological markers for AD

By far, only a few studies have been reported to explore the use of MOF materials for constructing biosensors to detect total tau protein and phosphorylated tau protein. One such study was conducted by Gu's research team in 2019. They synthesized an ultrathin 2D MOF, Hf-1,3,5-tris(4-carboxyphenyl)benzene (BTB) nanosheets [132], using a solvothermal method. By strictly regulating the hydrophobicity of the MOFs, the affinity of the metals, and the distance between adjacent metal clusters, the team was able to distinguish between monophosphopeptides and multiphosphopeptides. They were also able to differentiate monophosphopeptides from non-phosphopeptides under acidic conditions by regulating the reaction conditions. Based on this design principle, they measured the amount of phosphorylated proteins and phosphopeptides in the cortical tissue of AD-associated mice with conditional knockout of protein kinase B (i.e., *Akt*) using liquid chromatography/tandem mass spectrometry (LC/MS/MS) Fig. 7**a**. The

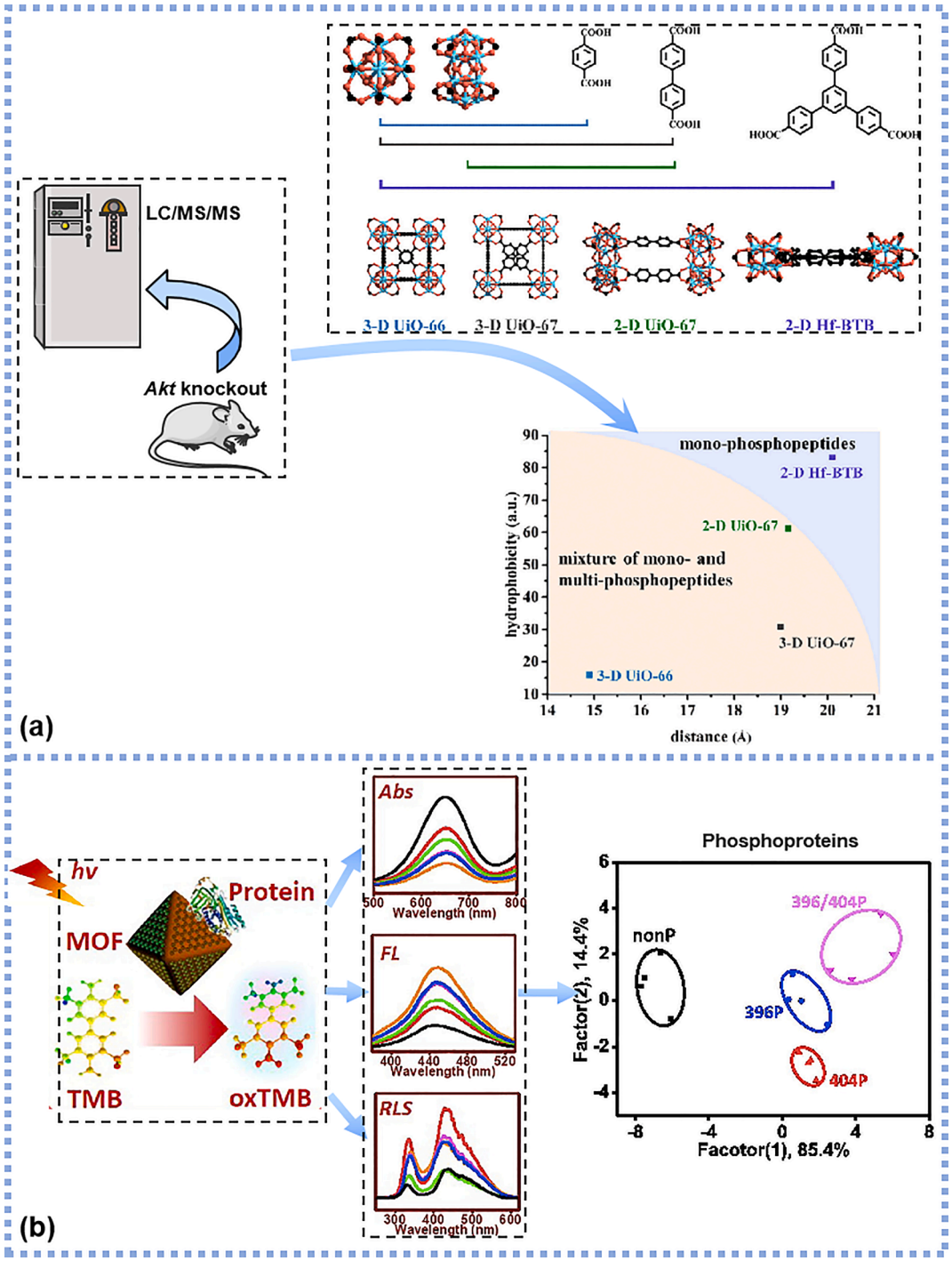

Fig. 7. MOF-based biosensors for detection of tau pathology markers. **(a)** Monophosphopeptides and polyphosphopeptides were distinguished on the basis of hydrophobicity, metal affinity and distance between adjacent metal clusters of the 2D Hf-BTB. Based on this design principle, 2D Hf-BTB enrichment allowed the identification of phosphoproteins and monophosphopeptides in *Akt* knockout mice. Reproduced with permission [132]. Copyright 2019 American Chemical Society. **(b)** Using changes in Abs, FL and RLS 3D spectral arrays, the MOF/TMB sensing system sensitively identifies and discriminates phosphoprotein patterns and protein phosphorylation distributions. Reproduced with permission [133]. Copyright 2021 Elsevier Inc.

results showed that a phosphoprotein and a monophosphopeptide were identified in the *Akt* knockout mice after 2D Hf-BTB enrichment, whereas no phosphopeptides and phosphoproteins were identified in the control mice.

Another existing study for tau-related biosensor was conducted by Chen et al. in 2021. They developed a MOF/TMB sensing system that utilizes changes in absorbance (Abs), fluorescence (FL), and resonance light scattering (RLS) 3D spectral arrays to sensitively identify and discriminate phosphoprotein patterns and protein phosphorylation distributions [133]. The team used a one-pot hydrothermal method to synthesize Zr-FeTCPP-MOF composites by coordinating Zr_6 clusters with 2-aminoterephthalic acid (NH_2-BDC) and Fe(III) mesotetra(4-carboxyphenyl)porphine chloride (FeTCPPCl). The composites combine the adsorption capacity of Zr-MOF, the fluorescence behavior of NH_2-BDC, and the biomimetic enzymatic activity of FeTCPPCl. The strong affinity between Zr-MOF and phosphate groups can be exploited to trap phosphoproteins. The FeTCPPCl component can oxidize TMB to a blue product, oxTMB), which can quench NH_2-BDC-mediated FL. However, the adsorbed phosphoproteins can inhibit the oxidation of TMB by the MOF, leading to changes in oxTMB Abs and FL of Zr-FeTCPP-MOF. Additionally, the presence of TMB and adsorbed phosphoprotein on the surface leads to an increase in MOF/phosphoprotein particle size, resulting in enhanced RLS signaling. Using this system, the team successfully identified four tau peptides with different levels and phosphorylation sites including non-phosphorylated, single phosphorylation of Ser396 or Ser404, and both Ser396 and Ser404 phosphorylations (Fig. 7**b**). Given the crucial role of tau proteins in AD pathophysiology, it is likely that more MOF-based biosensing platforms will emerge in the future to enable more sensitive, easier, and cheaper tau detection.

5.1.3. Other pathological markers for AD

While neurotoxic Aβ and tau are the typical markers for determining AD, other markers have also been observed. Presenilin 1 is essential for neuronal growth and maturation, and mutations in its gene sequence predispose individuals to familial AD. ThT can bind to DNA sequences and the assembly of G-quadruplex/ThT can emit a strong fluorescent signal, making it a useful G-quadruplex binder. ThT@Er-MOF [130] was used by the Ding team to detect presenilin 1 based on a label-free split-fluorescence Apt method. Since SSODN is a mutation-prone DNA sequence part of presenilin 1, detection of SSODN was chosen to indirectly reflect presenilin 1 levels. The guanine (G)-rich split SSODN Apts (SSODN-P1 and SSODN-P2) increased the fluorescence intensity of ThT by specifically binding to ThT, enabling the detection of the target SSODN. The ThT@Er-MOF-based aptasensor showed a linear range of 0–33 nM and a LOD of 0.517 pM.

The loss of basal forebrain cholinergic neurons in AD patients results in an imbalance in acetylcholine (Ach) metabolism, which impacts various aspects of cognition and behavior [139]. Therefore, it is crucial to develop simple, inexpensive, stable, and sensitive detection systems for monitoring Ach levels in AD patients. Toward this end, the Hwang team synthesized TMBDA-MIL-100(Fe) by post-synthetically modifying the coordinatively unsaturated metal sites (CUS) of MIL-100(Fe) grafted with N,N,N′,N′-tetramethyl-1,4-butanediamine (TMBDA). This material was used to create a fluorescent sensor for detecting choline (Cho) and Ach [134]. The amine-functionalized TMBDA-MIL-100(Fe) exhibits strong peroxidase-mimetic activity and can catalyze H_2O_2 oxidation due to the synergistic effect of increased negative surface charge and control of the size of the grafted diamine molecule. TMBDA-MIL-100(Fe) binds to specific enzymes (choline oxidase and acetylcholinesterase (AChE)) that catalyze Cho and Ach to produce H_2O_2 by sequentially catalyzing the oxidation of Ach. TMBDA-MIL-100(Fe) was activated to oxidize the fluorescent substrate Amplex UltraRed, resulting in a strong fluorescent signal. Using the milk assay, a good linear relationship between fluorescence intensity and Ach concentration was observed in the range of 0.5–10 μM, with a LOD of 0.027 μM and 100 % recovery. When serum samples were assayed, a linear relationship between fluorescence intensity and Ach concentration was found in the range of 0.1–10 μM, with a LOD of 0.036 μM and a recovery of 97–103 %. Another study targeting Ach detection was conducted by the team of Ding and Wang [130]. They designed ThT@Er-MOF as a fluorescent sensor, which exhibited excellent binding ability for Ach, particularly after the addition of acetylcholine esterase medium, which attracted more Ach and greatly improved the sensitivity of Ach detection. The fluorescence intensity was linearly related to the Ach concentration in the range of 0–8 nM, corresponding to a LOD value of 0.03226 nM.

AChE is also considered to be a diagnostic biomarker for AD. AChE activity controls the degradation of Ach and therefore the detection of AChE activity is important for the early diagnosis of AD. Ultra-thin 2D MOF NSs with peroxidase activity catalyze the oxidation of TMB to blue ox-TMB by H2O2. AChE catalyzes the acetylthiocholine (ATCh) substrate to produce thiocholine (TCh), which interferes with the peroxidase activity of 2D MOF NSs and reduces the production of ox-TMB. Based on this principle, ultrathin 2D copper-catecholate (Cu-CAT) NSs [135] and Zn-TCPP(Fe) NSs [136] have been used for the quantitative detection of AChE activity. The sensitivity of Cu-CAT NSs and Zn-TCPP (Fe) NSs for the detection of AChE activity was evaluated by colorimetric and the results showed that the Cu-CAT NSs had a wide range of concentrations for the detection of AChE activity in human serum from 0.01 to 4.0 mU/mL with an LOD of 0.01 mU/mL and a recovery of 93.00–101.00 %. However, the linear concentration range of Zn-TCPP (Fe) NSs for the detection of AChE was 0.54–3.93 mU/mL with an LOD of 0.029 mU/mL, and its recovery was 96.99–101.10 %.

5.2. MOFs for AD treatment

There are a limited number of clinically approved drugs currently available for the treatment of AD. Their efficacy is often poor, mainly serving to improve symptoms or delay disease progression. Treatment is also further hindered by the fact that the BBB restricts drug permeability, leading to reduced drug concentrations in the brain. Consequently, there is an urgent need to identify novel drug carriers with good BBB permeability. In recent years, nanotechnology has emerged as a promising approach and a possible answer for the treatment of AD, as nanocarriers can overcome BBB limitations to target specific brain regions or cells and enable multi-target therapy. MOFs specifically have emerged as an ideal drug carrier due to their flexible size and structure, their ability to carry multifunctional sites, and can be designed at the nanoscale. These attributes can be leveraged, making MOFs ideal platforms for the treatment of diseases like AD and have led to their increasing implementation throughout the medical field. In the following section, we focus on the therapeutic effects of MOF-based drug carriers targeting different AD pathologies (Fig. 8, Table 2) and review the biocompatibility of MOF-associated materials (Table 2).

5.2.1. Targeting Aβ for AD treatment

Aβ deposition is recognized by the scientific community as the key pathological feature of AD. Targeting brain tissue with MOF materials to inhibit the metabolic process of Aβ aggregation is expected to provide a new perspective for the treatment of AD. Liu's team utilized hydrophilic PEG-NH_2 to modify the surface of MIL-101(Fe), composed of inorganic $FeCl_3{\cdot}6H_2O$ and organic ligand terephthalic acid (TPA) to enhance its biocompatibility [140]. The modified MIL-101 has a large positive charge and can combine with negatively charged Au NPs to form a nanoscale MOF (NMOF) composite (AuNPs@PEG@MIL-101). This NMOF displayed the ability to adsorb a significant amount of $A\beta_{40}$ and uniformly bind it on its surface. By inhibiting $A\beta_{40}$ aggregation and promoting the degradation of Aβ protofibrils, the composite can prevent neuronal apoptosis while preserving the integrity of the cell membrane and microtubule structure (Fig. 9). The composite was found to be non-toxic and significantly reversed $A\beta_{40}$-induced cell death.

PDT is a new non-invasive method of treating disease with laser-activated photosensitive drugs [143]. In recent years, it has attracted

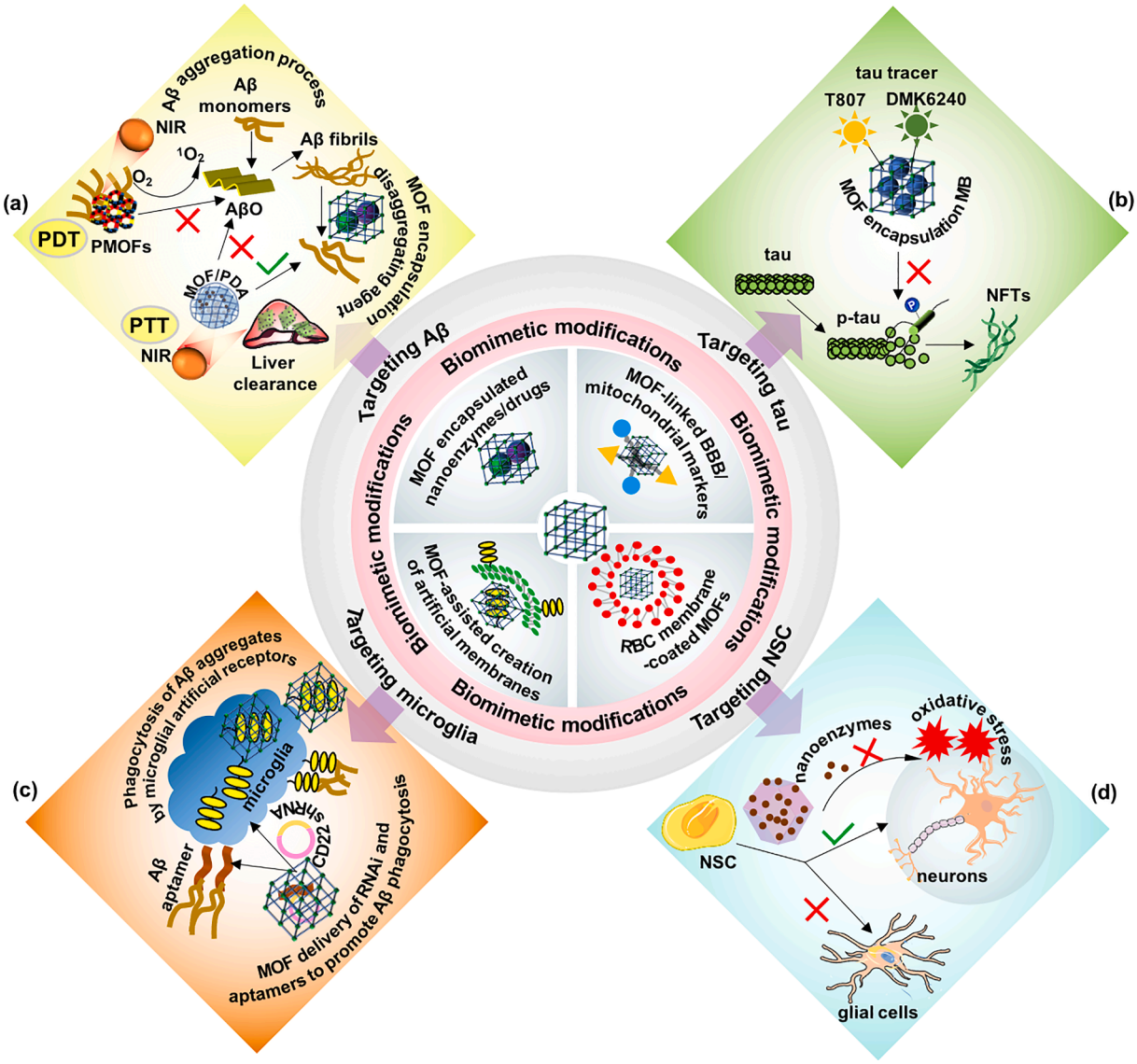

Fig. 8. MOF-based drug carriers for AD treatment. In order to improve the biocompatibility and bioavailability of MOFs, biomimetic modifications were made to MOFs such as wrapping MOFs with nanoenzymes, linking MOFs to BBB or mitochondrial markers, surface-wrapping MOFs with RBC membranes, and assisting in the construction of artificial microglial membranes. **(a)** Targeting Aβ for AD treatment. Current MOF-associated research aimed at treating Aβ pathology revolves around the ideas of inhibiting Aβ aggregation (using PDT, PTT), promoting Aβ plaque cleavage (using lytic agents, PTT) and promoting Aβ clearance through the liver system. **(b)** Targeting tau for AD treatment. With the help of tau indicator T807 and DMK6240, MB selectively binds tau proteins with high affinity and inhibits tau protein aggregation. **(c)** Targeting microglia for AD treatment. Engineering microglial membranes or silencing the AD risk gene CD22 facilitates Aβ phagocytosis by microglia. **(d)** Targeting NSC for AD treatment. MOF-based drug carriers encapsulating regulatory factors that inhibit glial cell differentiation promote NSC differentiation into neurons.

more attention in the field of AD therapy. Photo-oxidation is an effective photodynamic method for converting Aβ into an oxidized form to inhibit its aggregation [33,36]. The complex structure of human tissues limits the penetration depth of light due to its absorption by biological tissues upon entry into the body. Therefore, the penetration of light into brain tissue through the skull has been a challenge for photodynamic therapy in the field of neuroscience. It has been discovered that the absorption of light by biological tissue is significantly reduced in the 700–900 nm wavelength range of near-infrared (NIR) light, enabling NIR light to penetrate the skull and reach the cerebral cortex [144]. The cerebral cortex is the primary site of Aβ deposition in AD patients, so photo-oxidation based on NIR irradiation may enhance the inhibitory effect on Aβ aggregation. Some NPs have been shown to be excellent Aβ photosensitizers, overcoming the limitations of small molecule photosensitizers such as thioflavin T derivatives and riboflavin which tend to aggregate with high photo-oxidation efficiency and low biotoxicity. Porphyrinic MOFs (PMOFs) are an excellent class of Aβ photosensitizers. The aromatic rings and exposed metal sites found in these MOFs can enrich Aβ for efficient photo-oxidation. For example, Zirconium PCN-224 NPs ligated with tetra-kis(4-carboxyphenyl)porphyrin (TCPP) have a fluorescence quantum yield of 17 % and high photo-oxidation efficiency and have been reported to inhibit the self-assembly of $A\beta_{42}$ monomers and $A\beta_{42}$-induced cytotoxicity by generating singlet oxygen ($^1O_2$) under 650 nm NIR irradiation (Fig. 10**a**) [39]. The NPs are biocompatible, and MTT showed PC12 cell viability of over 80 % even at high concentrations of 100 μg/mL.

PMOFs not only avoid aggregation but also possess the ability to chelate metals. Based on this, Qu's team selected Hf-MOFs as an efficient Aβ photooxidant and used LPFFD peptide to modify Hf-MOFs to ensure Aβ targeting [33]. Hf-MOFs produced $^1O_2$ under 450 nm laser irradiation and photo-oxidized Aβ to prevent its self-aggregation. Additionally, the porphyrin structure of Hf-MOFs has a high affinity for Cu^{II}, and it

Table 2
MOF-associated materials for AD treatment.

MOF type	Role	Biocompatibility	Experimental subject		Target biomarker	Neuroprotective effect
			In vitro	In vivo		
ZIF-8 [127]	drug carrier, and chemo-photothermal synergistic therapy	SH-SY5Y and BV-2 maintained over 90 % cytoactivity after 48 h co-culture with ZIF-8 composite.	SH-SY5Y, BV-2	–	Aβ	Inhibition of Aβ monomer aggregation, promotion of Aβ fibril degradation and antioxidant.
MIL-101 (Fe) [140]	drug carrier	AuNPs@PEG@MIL-101 exhibited no cytotoxicity towards PC12 cells.	PC12	–	$Aβ_{40}$	Inhibition of $Aβ_{40}$ aggregation, promotion of Aβ fibril degradation and prevention of neuronal apoptosis.
Hf-MOFs [33]	drug carrier	LPFFD-modified Hf-MOF had no significant cytotoxicity to PC12 cells in the concentration range of 0–50 μg/mL.	PC12	*Caenorhabditiss elegans*	Aβ	Photo-oxidation of Aβ inhibited its self-aggregation and chelation of Cu^{II} inhibited Cu^{II}-mediated Aβ aggregation and neurotoxicity.
PCN-224 [39]	drug carrier	PC12 cell viability exceeded 80 % even at high PCN-224 concentrations of 100 μg/mL.	PC12	–	$Aβ_{42}$	Inhibition of self-assembly of $Aβ_{42}$ monomers and $Aβ_{42}$-induced cytotoxicity.
PCN-222 [40]	drug carrier	PC12 cells maintained over 90 % cell viability in up to 200 μg/ml of PCN-222 and PCN-222@ICG and low cytotoxicity in various concentrations of PCN-222@ICG for up to 72 h.	PC12	Ex Vivo AD Mouse Brain	$Aβ_{42}$	Inhibition of $Aβ_{42}$ aggregation and promotion of Aβ plaque dissociation.
Fe-MIL-88B-NH2 [38]	drug carrier, and bioimaging	Nanoscale MOFs were less cytotoxic and did not cause significant morphological changes in major organs. Maximum iron levels were reached on day 7, followed by a gradual decrease in concentration. H2BDC concentrations remained low throughout the week.	SH-SY5Y	SD rats	tau	Inhibition of p-tau protein aggregation and neuronal death and improvement of cognitive function in AD rats.
Zn-CA [141]	drug carrier, anticomplement activity, and biosensor	TR-ZRA did not cause any pathological changes in the major organs of the mice and was clearly biocompatible.	bEnd.3, HT22, and BV-2	APP/PS1 mouse	Aβ, microglia	Inhibition of CD22 expression and complement activation, and promotion of Aβ phagocytosis by microglia.
Mn-MOF [32]	drug carrier and biomimetic enzyme	Mn-MOFs were less cytotoxic and Mn-MOF did not cause abnormal neuronal apoptosis and major organ damage in mice. In addition, Mn and Zr ions decreased to normal control levels within two weeks.	BV-2	mouse	Aβ, microglia	Specific capture of Aβ and anti-oxidation.
MIL-100 (Fe) [142]	drug carrier and biomimetic enzyme	CeRMS is biodegradable and the iron is almost completely removed after 5 weeks of NSC transplantation.	NSC, PC12	3 × Tg AD mouse	NSC	Inhibition of oxidative stress and promotion of NSC differentiation into neurons.

inhibits Cu^{II}-mediated Aβ aggregation and neurotoxicity by chelating Cu^{II}. LPFFD-modified Hf-MOF also ameliorates paralysis and motor impairment and prolongs the lifespan of *Caenorhabditis elegans* CL2006, which expresses Aβ protein. Ultrathin 2D nanosheets of black phosphorus (BP) also serve as a NIR photocatalyst. It forms a BP@BTA nanoplatform with 4-(6-methyl-1,3-benzothiazol-2-yl)phenylamine (BTA), which has a high affinity for β-fold structural peptides [36]. Under NIR irradiation, BP@BTA inhibits the aggregation of Aβ by generating $^1O_2$ oxidation (Fig. 10**b**).

Combining NIR-based photo-oxidation with photothermal treatment can synergistically enhance the inhibition of Aβ aggregation. PTT is a new method of tumor treatment different from PDT [145], which kills tumor cells by converting light energy into heat, and in recent years it has been found to have great potential for the treatment of AD. When the 2D porphyrin PCN-222 is coordinated with TCPP and indocyanine green (ICG), it forms PCN-222@ICG and gains a photothermal effect through electrostatic adsorption [40]. Under 808 nm NIR light irradiation, PCN-222@ICG significantly inhibited $Aβ_{42}$ aggregation better than PCN-222, and PCN-222@ICG could control the structure of Aβ monomer below 100 nm. The CCK-8 results showed that PC12 cells remained above 90 % cell viability in up to 200 μg/mL of PCN-222 and PCN-222@ICG, and low cytotoxicity remained low at different concentrations of PCN-222@ICG for up to 72 h. PCN-222@ICG was shown increase its effectiveness by linking to rabies virus glycoprotein (RVG) (PCN-222@ICG@RVG), a protein that is widely expressed on the surface of brain endothelial cells and characteristically binds to the nicotinic acetylcholine receptor, thereby enhancing brain tissue targeting. NIR-activated PCN-222@ICG@RVG promoted the dissociation of Aβ plaques in brain tissue sections from ex vivo AD mice (Fig. 11**a**).

In view of the strong absorption of NIR by the photothermal agent PDA, Yu et al. innovatively developed a new approach based on MOF-encapsulated antioxidant herbal medicine combined with PDA photothermal synergistic treatment for AD [127]. Resveratrol (Res) is a natural polyphenol with multiple neuroprotective effects such as antioxidant and anti-inflammatory (26, 30), while ceria NPs (CeONP) also possess antioxidant activity and also mimic various biological enzymes such as SOD and catalase [146]. Res and CeONP doubly ensure inhibition of Aβ-mediated neuropathology. To enhance the bioavailability of Res, a phase-change material, PCM (tetradecanol), was chosen as an athermal response switch to control the release of Res. Res, CeONP and PCM were encapsulated in ZIF-8 pores by an in-situ encapsulation strategy, and then PDA was coated on the surface to form the CeONP-Res-PCM@ZIF-8/PDA composite nanomaterial. The results confirmed that CeONP-Res-PCM@ZIF-8/PDA exhibited multiple neuroprotective effects such as inhibition of Aβ monomer aggregation, degradation of Aβ fibrils and antioxidative stress (Fig. 11**b**). The cytotoxicity of CeONP-Res-PCM@ZIF-8/PDA on SH-SY5Y and BV-2 cells was evaluated in CCK-8 experiments and it was found that the cellular activity remained above 90 % after co-culture with the composite for 48 h.

Aside from MOFs, other nanomaterials have been found to promote Aβ accumulation in peripheral blood through photodynamic therapy, thereby enhancing Aβ uptake and clearance by the liver [34]. Additionally, these other nanomaterials can be encapsulated with anti-inflammatory herbs (e.g. resveratrol, curcumin) that inhibit Aβ aggregation [31]. In summary, current research targeting Aβ pathology in AD revolves around the following ideas: (1) antioxidant/anti-inflammatory

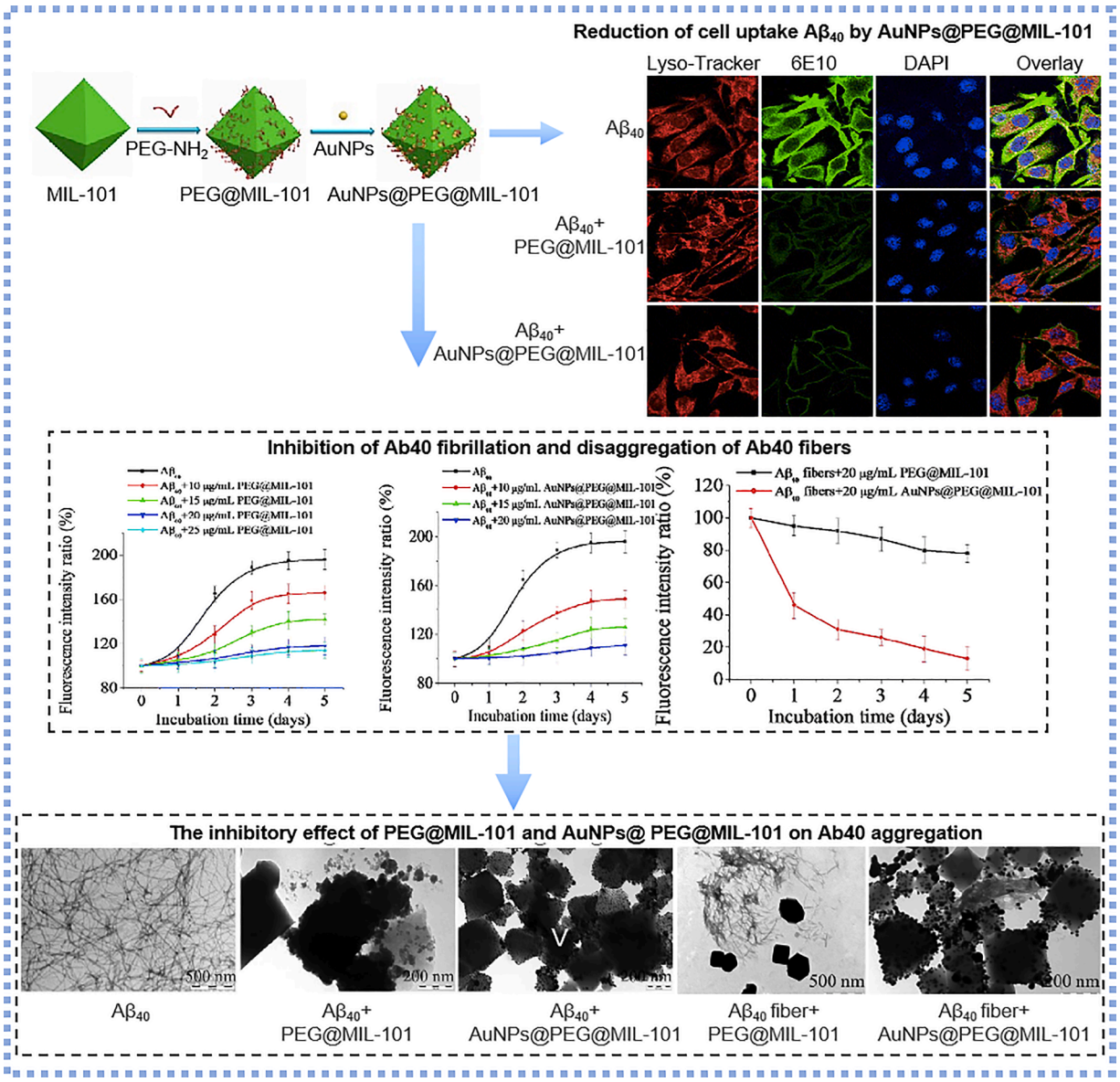

Fig. 9. AuNPs@PEG@MIL-101 attenuates Aβ neurotoxicity. As an Aβ inhibitor, AuNPs@PEG@MIL-101 can reduce cellular uptake of Aβ40 and Aβ40 aggregation, effectively inhibit extracellular Aβ monomer fibrillation and disrupt the preformed Aβ fibrils. Reproduced with permission [140]. Copyright The Royal Society of Chemistry 2023.

therapy (nanomimetic activity of nanoenzymes, herbs), (2) inhibition of Aβ aggregation (PDT, PTT), (3) promotion of Aβ plaque cleavage (lytic agents, PTT), and (4) promotion of Aβ clearance (central microglia, peripheral liver system). Given the multiple advantages of MOFs as drug delivery systems, the potential of targeting Aβ for AD treatment could be explored in the future from the multiple perspectives described above.

5.2.2. *Targeting tau for AD treatment*

Hyperphosphorylation and aggregation of tau proteins are core pathological features of AD, and therefore, therapeutic targeting of tau proteins has received much attention. The research in the pathology of this protein as it relates to AD has focused on (1) inhibiting tau protein hyperphosphorylation, (2) stabilizing microtubule structure, (3) inhibiting tau protein aggregation, (4) selectively binding tau protein aggregates, (5) blocking tau protein propagation, (6) promoting clearance of abnormal tau protein, and (7) inhibiting pathological tau protein-associated neurotoxicity. Unfortunately, there has been no successful translation of therapies targeting tau proteins based on this research into applications for clinical patients. To fill this gap, researchers have explored the feasibility of targeting tau pathology with MOF-related materials for the treatment of AD at a basic experimental level.

MB is a phenothiazine methylthionium chloride that selectively binds tau proteins with high affinity and inhibits tau protein aggregation [147]. Kong, Wang et al. similarly chose MB as a tau protein ligand to inhibit its aggregation. They constructed a nanoscale Fe-MIL-88B-NH_2 using a hydrothermal method and encapsulated MB in its cavity [38]. To improve the targeting of phosphorylated tau proteins, they chose the non-radioactive defluorinated 5-amino-3-(pyrrolo[2,3–c]pyridin-1-yl) isoquinoline (DMK6240) as the tau positron emission tomography tracer. Fe-MIL-88B-NH_2 was then post-synthetically modified with 1,4,7-triazacyclononane-1,4,7-triacetic acid (NOTA) and DMK6240 via NOTA grafting to form the Fe-MIL88B-NH_2−NOTA-DMK6240/MB composite encapsulated with MB. The relaxation value of Fe-MIL88B-NH_2−NOTA-DMK6240 showed a proportional change in relation to the iron concentration and had a similar effect on the contrast of the observed images. An experiment was then conducted using a rat model of AD with okadaic acid (OA)-induced tau protein hyperphosphorylation. The results showed that Fe-MIL88B-NH_2-NOTA-

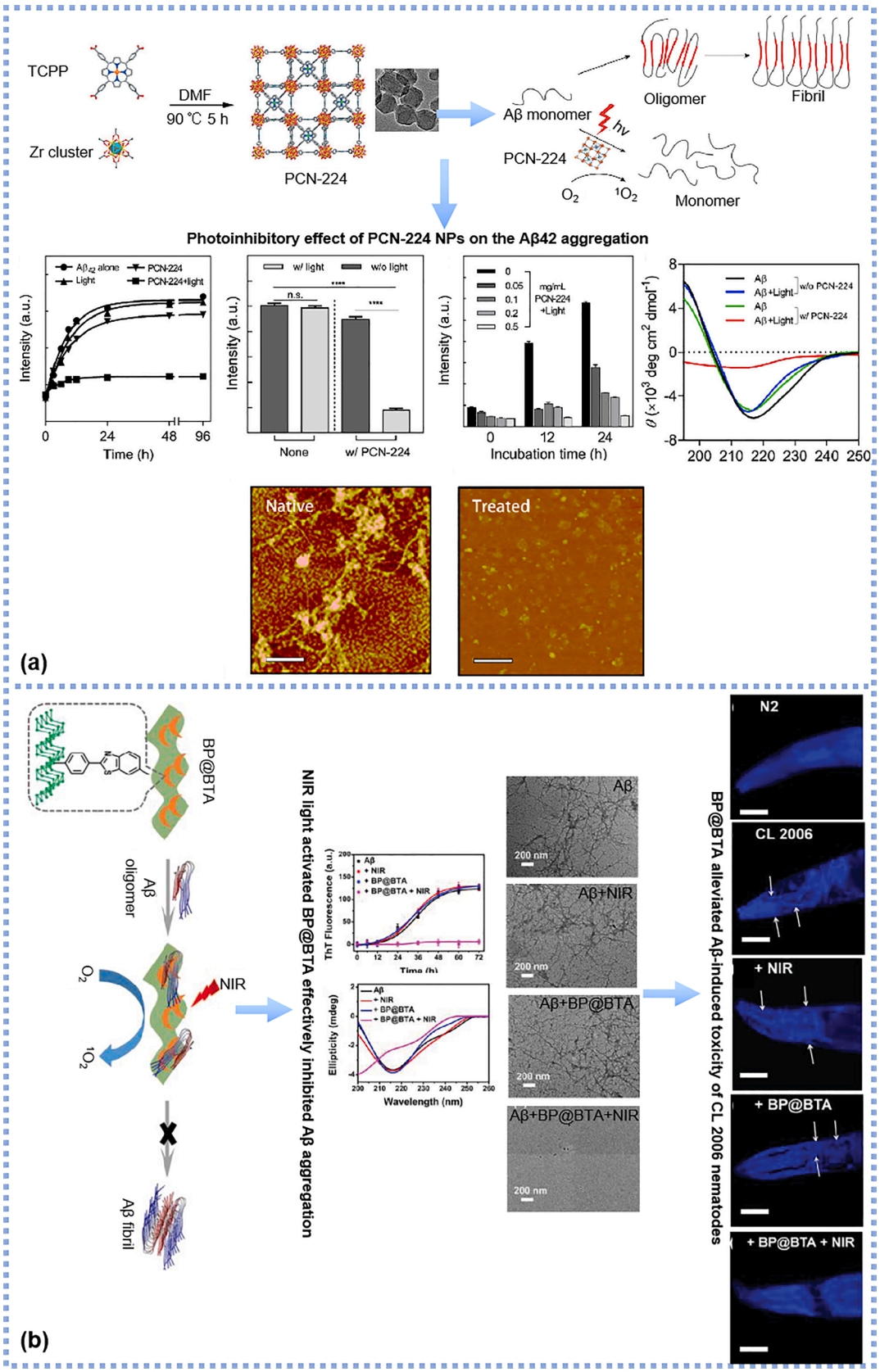

Fig. 10. MOF acts as an Aβ photooxidant to inhibit Aβ aggregation. **(a)** The photoinhibitory effect of PCN-224 NPs on the Aβ42 aggregation. Reproduced with permission [39]. Copyright 2018 American Chemical Society. **(b)** NIR-activated BP@BTA effectively inhibited Aβ aggregation and ameliorated Aβ-induced toxicity of CL 2006 nematodes. Reproduced with permission [36]. Copyright 2019 WILEY-VCH Verlag GmbH & Co.

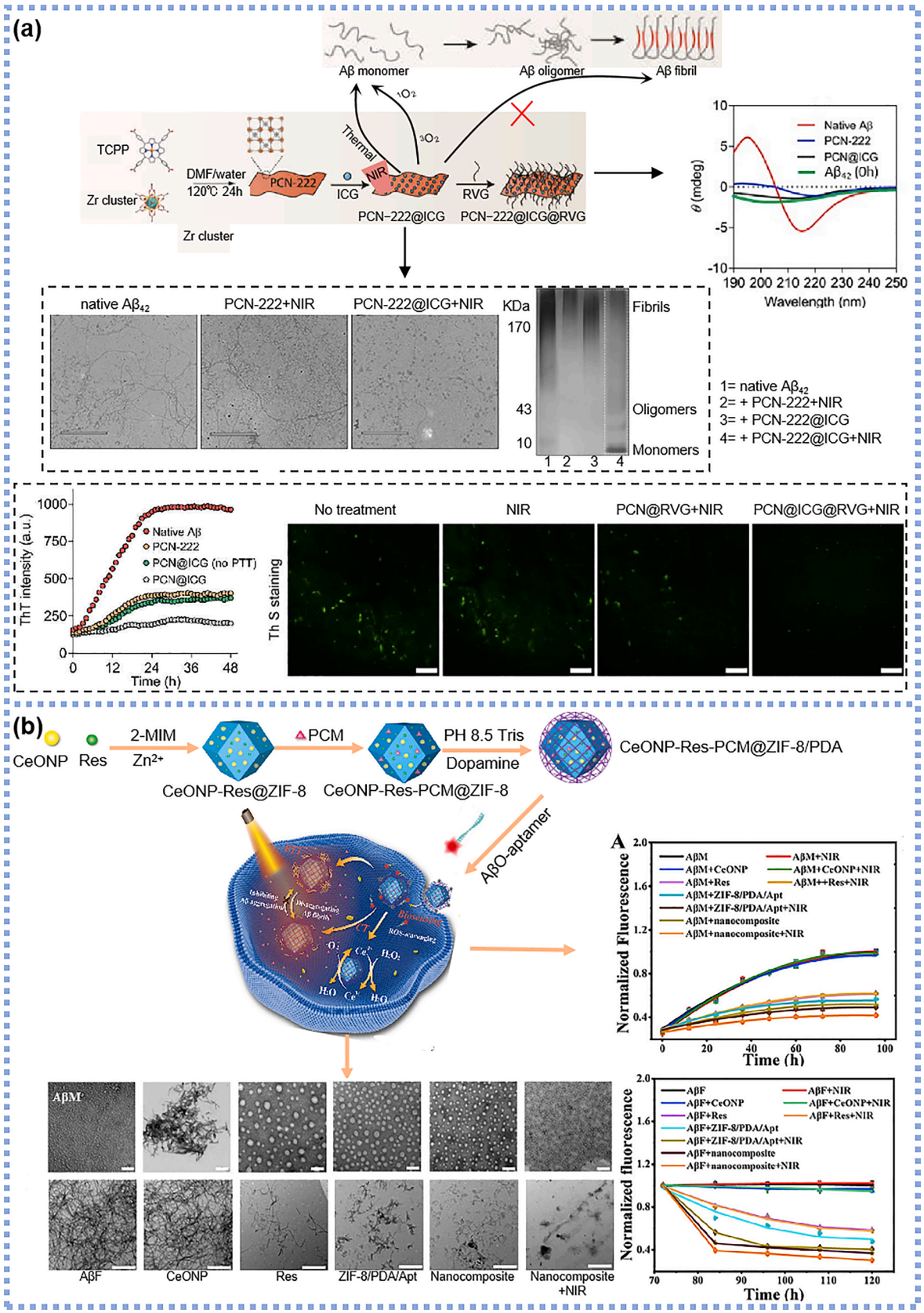

Fig. 11. MOF inhibits Aβ aggregation through the photothermal effect. **(a)** Schematic illustration of the synthesis of PCN-222@ICG and PCN-222@ICG@RVG. Photo-activated PCN-222 and PCN-222@ICG inhibit Aβ42 aggregation and promote Aβ plaque dissociation in ex vivo mouse brain. Reproduced with permission [40]. Copyright 2022 by the authors. **(b)** Schematic illustration of the synthesis of CeONP-Res-PCM@ZIF-8/PDA. CeONP-Res-PCM@ZIF8/PDA inhibition of Aβ monomer aggregation and degradation of Aβ fibrils. Reproduced with permission [127]. Copyright 2021 American Chemical Society.

DMK6240/MB could inhibit tau protein hyperphosphorylation and full-length 2N4R tau protein aggregation (Fig. 12), inhibit hippocampal neuronal death, and improve cognitive function in AD rats. Results from in vitro and in vivo toxicity studies showed that the material exhibits good biocompatibility with MTT detecting 71 % of SH-SY5Y cell activity. HE staining also showed no damage to hippocampus, heart, liver, spleen, and kidney tissues, and the material is degradable with iron content reaching a maximum on day 7 followed by a gradual decrease in concentration, while 2-aminoterephthalic acid (H_2BDC) concentration remained low throughout the week with little change observed.

In summary, current research into targeting tau pathology in AD has focused on both the production and metabolism of phosphorylated tau proteins. The "seeds of pathology" are cut off by inhibiting the phosphorylation of tau proteins. For phosphorylated tau proteins that are already produced, research aims to inhibit the aggregation of phosphorylated tau proteins and seeding between different cells. MOF-based materials have shown promise in targeting tau pathology. However, more research is needed to develop effective therapies targeting tau pathology in AD.

5.2.3. *Targeting other hallmarks for AD treatment*

In addition to MOFs-based drug carriers targeting Aβ and phosphorylated tau proteins, several studies have reported targeting other pathologies of AD, such as microglia and neural stem cells. Inappropriate activation of microglia deprives them of their ability to phagocytically clear Aβ, and in turn inhibits the mediation of ongoing neuroinflammation in the brain. Therefore, correcting the functional state of microglia, restoring their Aβ phagocytosis, and suppressing neuroinflammation are important for the treatment of AD. Qu's team successfully constructed an artificial Aβ receptor to induce microglia to engulf Aβ aggregates through receptor-mediated endocytosis by engineering microglial membranes [32]. Specifically, they used Mn-TCPP-linked Zr_6 clusters to form porous Mn-MOFs and encapsulated N-azidoacetylmannosamine (AcManNAz) within the Mn-MOFs (AcManNAz@Mn-MOFs, Az@MOF). The porous nature of the Mn-MOFs ensures slow release of the encapsulated AcManNAz, resulting in a long half-life of AcManNAz on microglial cell membranes. ThS (a thioflavine dye), which selectively captures Aβ, is then conjugated to AcManNAz by a click reaction. It should be noted that during the process of phagocytosis and clearance of Aβ, microglial cells are prone to excessive activation, which poses a potential risk of oxidative stress damage. However, Mn-TCPP exhibits enzymatic activities mimicking SOD and CAT, which can prevent secondary damage caused by excessive activation of microglial cells. Taken together, the ThS-linked Az@MOF not only has the ability to specifically scavenge Aβ, but also has both SOD and CAT mimetic enzymatic activities, both of which synergistically ensure that the microglia are in a neuroprotective subtype. TUNEL and HE stains showed that Mn-MOF did not cause abnormal neuronal apoptosis and major organ damage in mice. In addition, Mn and Zr ions decreased to normal control levels within two weeks.

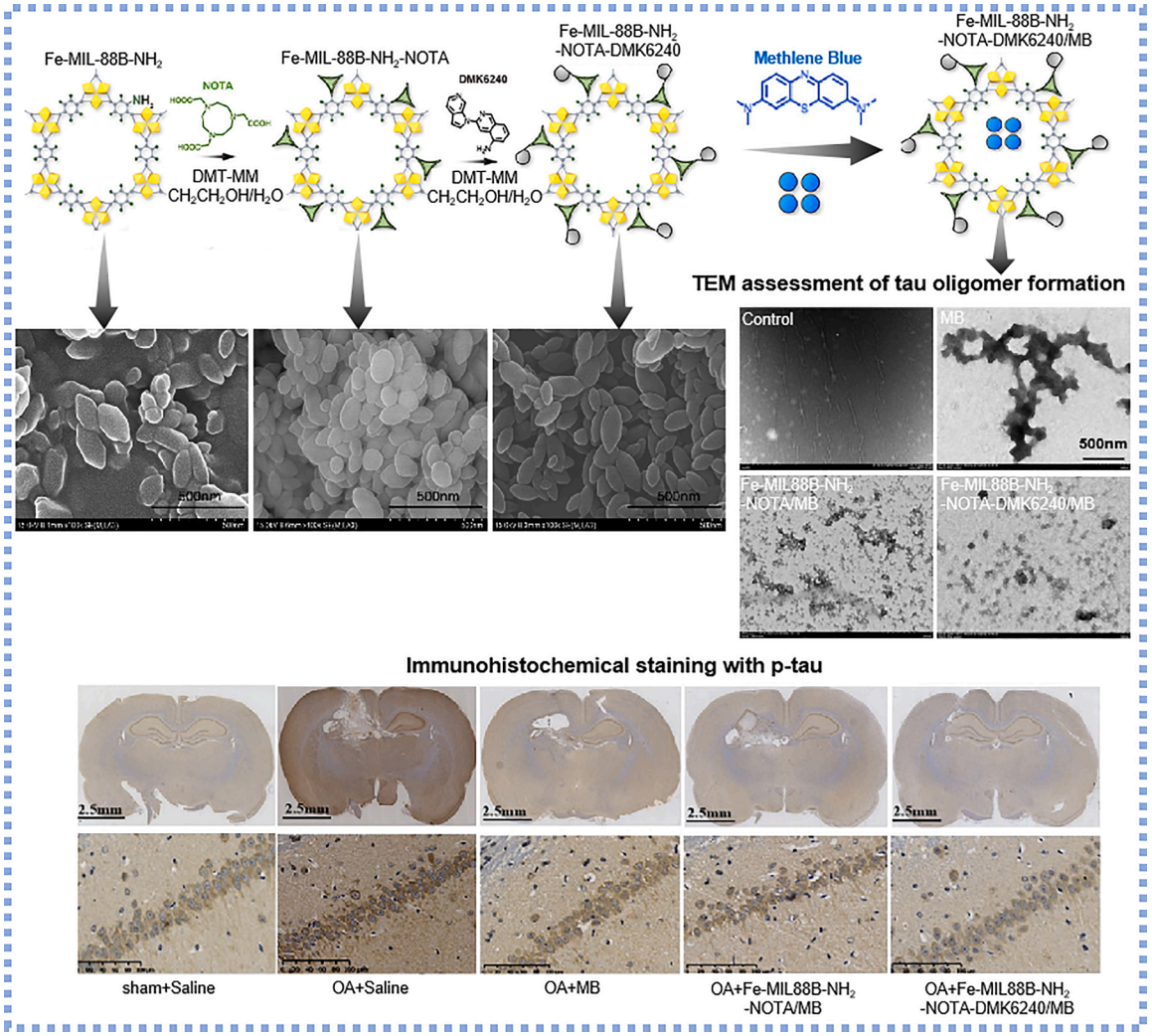

Fig. 12. Schematic illustration of the synthesis of Fe-MIL88B-NH2-NOTA-DMK6240/MB and its inhibition of tau protein hyperphosphorylation and aggregation. Reproduced with permission [38]. Copyright 2020 American Chemical Society.

Previous studies have shown that microglia express most of the risk genes associated with AD and CD22 expression is increased in senescent microglia [148]. Silencing CD22 could potentially enhance microglial phagocytosis of Aβ. MOF materials are a promising class of drug delivery carriers due to their high porosity and large specific surfaces, which can adsorb plasmid DNA through non-covalent interactions to prevent degradation. Chlorogenic acid (CA) is a phenolic acid with antibacterial, anti-inflammatory, and complement-activating properties. Nie and Li incorporated this moiety into a Zn-CA MOF (ZC) composed of Zn^{2+} and CA [141] loaded with CD22, shRNA (RNAi), and Aβ Apt (AAP) to form ZC/RNAi/AAP (ZRA) nanocores. The multifunctionalized ZRA not only acted as a drug delivery vehicle but also enabled biosensing of brain Aβ levels and Aβ plaque localization. To enhance BBB permeability and prolong in vivo half-life, the researchers introduced transferrin receptor (TfR) Apt onto the surface of erythrocyte membrane vesicles (RBCm) (TfR Apt-RBCm, TR) and then wrapped ZRA to form the TR-ZRA nanodrug system. TR-ZRA not only promoted microglial phagocytosis of Aβ by inhibiting CD22 expression but also had a neuroprotective effect by inhibiting complement activation via CA and showed that it was biocompatible, not causing any pathological damage to major organs.

Cognitive impairment in AD patients is ultimately caused by massive neuronal loss [149]. Therefore, neural stem cell (NSC) transplantation has gained attention as a potential treatment for AD. Qu et al. utilized the biocompatible MIL-100 (Fe) as a drug carrier to deliver small interfering RNA (siSOX9) and retinoic acid (RA) to NSCs [142]. The high porosity of MIL-100 (Fe) can accommodate both siSOX9 and RA while protecting siSOX9 from external interference. Additionally, NSCs are susceptible to oxidative stress during transplantation and differentiation, so ceria NPs with antioxidant effects were loaded into MIL-100(Fe). Together, MIL-100(Fe), ceria NPs, RA, and siSOX9 formed the CeNPs/RA@MIL-100/siSOX9 (CeRMS) nanocomposite. Results showed that CeRMS was efficiently internalized by NSCs and promoted NSC differentiation into neurons. In vivo experiments using triple transgenic (3 × Tg) AD mice demonstrated that CeRMS improved cognitive function in AD mice. CeRMS was biodegradable, and iron was almost completely cleared after 5 weeks of NSC transplantation.

6. Conclusions and perspectives

The application of MOFs in the biomedical field is expanded by the combination of advantages of nanoscale MOF materials and other functionalized materials. Problems such as BBB restriction, off-target effects, and immunogenicity induction are overcome by MOFs, making them excellent candidate carriers for drug delivery systems. In addition, precise design of nanoscale probes improves the accuracy and LOD of MOF sensors, enabling ultra-sensitive detection of biomarkers. Despite the broad prospects for the application of MOFs in AD diagnosis and treatment, there still exist significant challenges in their clinical utilization: [1] The biological safety of MOFs is the most pressing issue that needs to be addressed in clinical research. Given the rich diversity in the structure and types of MOFs, along with the complexity of the biological environment, accurately assessing the toxicity and biocompatibility of MOFs is a long-term and challenging task. In the evaluation process, it is imperative to comprehensively consider various aspects of MOFs, such as their synthesis components, functional design, synthesis conditions, chemical properties, size, and surface characteristics, to ensure thorough and rigorous consideration of their biological safety. Additionally, not only short-term or acute toxicity assessment is necessary, but long-term monitoring of potential risks of chronic toxicity from MOFs is essential to guarantee their absolute safety in clinical applications. [2] Regarding the metabolic pathways of MOFs within the human body, there is currently a lack of clear understanding. Although animal experiments have partially revealed the elimination pathways of MOFs in the body and the absorption, distribution, metabolism, and excretion processes in various tissues, these findings cannot entirely represent the actual situation in the human body due to insufficient research evidence based on human studies. In further research and applications, the drug administration routes of MOFs and factors such as their degradability, stability, blood half-life in the circulatory system need to be thoroughly considered to ensure their safety and efficacy in the human body. [3] The stability of MOFs in biological systems needs to be improved. Given the complex and variable human body environment, ensuring the structural and functional stability of MOFs within it poses a significant challenge. Particularly in the acidic environment of the human stomach acid, whether the structure of MOFs can remain stable and the reactions of their components under acidic conditions are currently unknown. These are crucial aspects that need to be deeply researched and explored. [4] Targeted delivery and precise control of drug release with MOFs present significant difficulties. Achieving this goal requires intricate and complex modification methods, relying on precise cooperation among the various components within MOFs. However, any minor error in this process could lead to targeting failures or unstable drug release control, thereby affecting therapeutic outcomes. [5] The large-scale production of MOFs currently faces multiple challenges, including stringent synthesis conditions, specific functionalization requirements, demands for structural stability, and high production costs. These combined factors hinder the development of economically efficient methods for synthesizing and functionalizing MOFs, impeding the industrialization process of MOFs.

The focus of this review is to summarize the relevant research on MOFs as biosensors and drug delivery carriers for the diagnosis and treatment of AD. MOFs have been utilized as biosensors to target the detection of biomarkers such as Aβ peptides or oligomers, phosphorylated tau protein, presenilin 1, BACE1, and neurotransmitters. These sensors overcome the limitations of low efficiency and poor thermal stability, exhibiting highly sensitive detection capabilities and high recovery rates in CSF and peripheral blood samples. The MOF-based biosensing platforms are operationally simple, cost-effective, and easily applicable in clinical settings, enabling reliable detection of biomarkers in the early pathological stages of AD. This highlights the future prospects of MOFs in the field of AD. Additionally, nanoscale MOF carriers can overcome the BBB restrictions, target specific brain regions or cells, and achieve multi-targeted therapies. They can also carry multifunctional sites based on therapeutic needs, combining with nanomaterials that possess anti-inflammatory and antioxidant properties. Furthermore, they can simultaneously deliver multiple drugs. These advantages make MOFs highly competitive as ideal drug carriers. This review particularly focuses on the therapeutic effects of MOF-based drug carriers targeting different pathological aspects of AD. The targeting of Aβ pathology involves inhibiting Aβ aggregation, promoting Aβ plaque degradation, and enhancing Aβ clearance. Meanwhile, targeting tau pathology is centered around studying the production and metabolism of phosphorylated tau protein, aiming to disrupt the “pathological seeds” by inhibiting tau protein phosphorylation. In the case of already produced phosphorylated tau protein, research is focused on inhibiting its aggregation and intercellular propagation. In addition to targeting Aβ and tau pathology, there are studies aimed at reversing the dysfunction of microglial cells and attempting NSC transplantation. These research findings demonstrate the promising therapeutic effects of MOF-based drug carriers, as well as their high biocompatibility and biosafety. In conclusion, we believe that with the continuous development of MOF synthesis technology and deeper research in AD pathology, MOFs have the potential for clinical translation in the near future, providing new opportunities for precise and individualized diagnosis and treatment of AD.

Declaration of competing interest

The authors declare that they have no known competing financial interests or personal relationships that could have appeared to influence the work reported in this paper.

Data availability

Data will be made available on request.

Acknowledgements

This study was supported by the General Program of the National Natural Science Foundation of China (82071442), the Jilin Provincial Department of Finance (JLSWSRCZX2021-004), Doctor of excellence program (DEP), The First Hospital of Jilin University (JDYY-DEP-2022015), Youth Development Fund, The First Hospital of Jilin University (JDYY14202338), and the Robert A. Welch Foundation (B-0027).

References

[1] WHO. Risk reduction of cognitive decline and dementia: WHO guidelines 2019 [Available from: https://www.who.int/publications/i/item/9789241550543.
[2] ADI. World Alzheimer Report 2022: Life after diagnosis: Navigating treatment, care and support. 2022 [Available from: https://www.alzint.org/resource/world-alzheimer-report-2022/.
[3] M. Goedert, M.G. Spillantini, A century of Alzheimer's disease, Science 314 (5800) (2006) 777–781.
[4] G. Livingston, J. Huntley, A. Sommerlad, D. Ames, C. Ballard, S. Banerjee, et al., Dementia prevention, intervention, and care: 2020 report of the Lancet Commission, Lancet 396 (10248) (2020) 413–446.
[5] W.J. Ray, V. Buggia-Prevot, Novel targets for Alzheimer's Disease: A view beyond amyloid, Annu. Rev. Med. 72 (2021) 15–28.
[6] K.S. Heavener, E.M. Bradshaw, The aging immune system in Alzheimer's and Parkinson's diseases, Semin. Immunopathol. 44 (5) (2022) 649–657.
[7] M. Jorfi, A. Maaser-Hecker, R.E. Tanzi, The neuroimmune axis of Alzheimer's disease, Genome Med. 15 (1) (2023) 6.
[8] H.C. Zhou, J.R. Long, O.M. Yaghi, Introduction to metal-organic frameworks, Chem. Rev. 112 (2) (2012) 673–674.
[9] I.B. Vasconcelos, T.G. Silva, G.C.G. Militão, T.A. Soares, N.M. Rodrigues, M. O. Rodrigues, et al., Cytotoxicity and slow release of the anti-cancer drug doxorubicin from ZIF-8, RSC Adv. 2 (25) (2012) 9437–9442.
[10] J. Yang, Y.W. Yang, Metal–organic frameworks for biomedical applications, Small 16 (2020) 10.
[11] L. Jiao, J.Y.R. Seow, W.S. Skinner, Z.U. Wang, H.-L. Jiang, Metal–organic frameworks: Structures and functional applications, Mater. Today 27 (2019) 43–68.
[12] T. Rezaee, R. Fazel-Zarandi, A. Karimi, A.A. Ensafi, Metal–organic frameworks for pharmaceutical and biomedical applications, J. Pharm. Biomed. Anal. 221 (2022) 115026.
[13] N.T.T. Nguyen, T.T.T. Nguyen, S. Ge, R.K. Liew, D.T.C. Nguyen, T.V. Tran, Recent progress and challenges of MOF-based nanocomposites in bioimaging, biosensing and biocarriers for drug delivery, Nanoscale Adv. 6 (7) (2024) 1800–1821.
[14] S. Sadiq, S. Khan, I. Khan, A. Khan, M. Humayun, P. Wu, et al., A critical review on metal-organic frameworks (MOFs) based nanomaterials for biomedical applications: Designing, recent trends, challenges, and prospects, Heliyon. 10 (3) (2024) e25521.
[15] S. Yu, K. Xu, Z. Wang, Z. Zhang, Z. Zhang, Bibliometric and visualized analysis of metal-organic frameworks in biomedical application, Front. Bioeng. Biotechnol. 11 (2023) 1190654.
[16] N. Stock, S. Biswas, Synthesis of metal-organic frameworks (MOFs): routes to various MOF topologies, morphologies, and composites, Chem. Rev. 112 (2) (2012) 933–969.
[17] H.W. Langmi, J. Ren, B. North, M. Mathe, D. Bessarabov, Hydrogen storage in metal-organic frameworks: a review, Electrochim. Acta 128 (2014) 368–392.
[18] H.-L. Jiang, T.A. Makal, H.-C. Zhou, Interpenetration control in metal–organic frameworks for functional applications, Coord. Chem. Rev. 257 (15) (2013) 2232–2249.
[19] H. Furukawa, K.E. Cordova, M. O'Keeffe, O.M. Yaghi, The chemistry and applications of metal-organic frameworks, Science 341 (6149) (2013) 1230444.
[20] P.Z. Moghadam, A. Li, X.W. Liu, R. Bueno-Perez, S.D. Wang, S.B. Wiggin, et al., Targeted classification of metal-organic frameworks in the Cambridge structural database (CSD), Chem. Sci. 11 (32) (2020) 8373–8387.
[21] D.J. O'Hearn, A. Bajpai, M.J. Zaworotko, The "Chemistree" of porous coordination networks: taxonomic classification of porous solids to guide crystal engineering studies, Small 17 (22) (2021) e2006351.
[22] L.E. Kreno, J.T. Hupp, R.P. Van Duyne, Metal-organic framework thin film for enhanced localized surface plasmon resonance gas sensing, Anal. Chem. 82 (19) (2010) 8042–8046.
[23] X. Ge, R. Wong, A. Anisa, S. Ma, Recent development of metal-organic framework nanocomposites for biomedical applications, Biomaterials 281 (2022) 121322.
[24] Y. Chen, Z. Yang, H. Hu, X. Zhou, F. You, C. Yao, et al., Advanced metal-organic frameworks-based catalysts in electrochemical sensors, Front. Chem. 10 (2022) 881172.
[25] Y. Guo, Y. Li, S. Zhou, Q. Ye, X. Zan, Y. He, Metal-Organic framework-based composites for protein delivery and therapeutics, ACS Biomater. Sci. Eng. 8 (10) (2022) 4028–4038.
[26] Y. Han, X. Chu, L. Cui, S. Fu, C. Gao, Y. Li, et al., Neuronal mitochondria-targeted therapy for Alzheimer's disease by systemic delivery of resveratrol using dual-modified novel biomimetic nanosystems, Drug Deliv. 27 (1) (2020) 502–518.
[27] X. Cai, Z. Xie, D. Li, M. Kassymova, S.-Q. Zang, H.-L. Jiang, Nano-sized metal-organic frameworks: Synthesis and applications, Coord. Chem. Rev. (2020) 417.
[28] S. Reyes-Esteves, J. Nong, P.M. Glassman, S. Omo-Lamai, S. Ohashi, J. W. Myerson, et al., Targeted drug delivery to the brain endothelium dominates over passive delivery via vascular leak in experimental intracerebral hemorrhage, J. Control Release 356 (2023) 185–195.
[29] O.A. Marcos-Contreras, C.F. Greineder, R.Y. Kiseleva, H. Parhiz, L.R. Walsh, V. Zuluaga-Ramirez, et al., Selective targeting of nanomedicine to inflamed cerebral vasculature to enhance the blood-brain barrier, Proc. Natl. Acad. Sci. USA 117 (7) (2020) 3405–3414.
[30] C. Li, N. Wang, G. Zheng, L. Yang, Oral administration of resveratrol-selenium-peptide nanocomposites alleviates Alzheimer's disease-like pathogenesis by inhibiting abeta aggregation and regulating gut microbiota, ACS Appl. Mater. Interfaces. 13 (39) (2021) 46406–46420.
[31] S. Fan, Y. Zheng, X. Liu, W. Fang, X. Chen, W. Liao, et al., Curcumin-loaded PLGA-PEG nanoparticles conjugated with B6 peptide for potential use in Alzheimer's disease, Drug Deliv. 25 (1) (2018) 1091–1102.
[32] D. Yu, C. Liu, H. Zhang, J. Ren, X. Qu, Glycoengineering artificial receptors for microglia to phagocytose Abeta aggregates, Chem. Sci. 12 (13) (2021) 4963–4969.
[33] D. Yu, Y. Guan, F. Bai, Z. Du, N. Gao, J. Ren, et al., Metal-organic frameworks harness Cu chelating and photooxidation against amyloid beta aggregation in vivo, Chemistry 25 (14) (2019) 3489–3495.
[34] M. Ma, Z. Liu, N. Gao, K. Dong, Z. Pi, L. Kang, et al., Near-infrared target enhanced peripheral clearance of amyloid-beta in Alzheimer's disease model, Biomaterials 276 (2021) 121065.
[35] L. Zhu, L. Xu, X. Wu, F. Deng, R. Ma, Y. Liu, et al., Tau-targeted multifunctional nanoinhibitor for Alzheimer's disease, ACS Appl. Mater. Interfaces. 13 (20) (2021) 23328–23338.
[36] Y. Li, Z. Du, X. Liu, M. Ma, D. Yu, Y. Lu, et al., Near-infrared activated black phosphorus as a nontoxic photo-oxidant for Alzheimer's amyloid-beta peptide, Small 15 (24) (2019) e1901116.
[37] Q. Chen, Y. Du, K. Zhang, Z. Liang, J. Li, H. Yu, et al., Tau-targeted multifunctional nanocomposite for combinational therapy of Alzheimer's disease, ACS Nano 12 (2) (2018) 1321–1338.
[38] J. Zhao, F. Yin, L. Ji, C. Wang, C. Shi, X. Liu, et al., Development of a tau-targeted drug delivery system using a multifunctional nanoscale metal-organic framework for Alzheimer's disease therapy, ACS Appl. Mater. Interfaces. 12 (40) (2020) 44447–44458.
[39] J. Wang, Y. Fan, Y. Tan, X. Zhao, Y. Zhang, C. Cheng, et al., Porphyrinic metal-organic framework PCN-224 Nanoparticles for near-infrared-induced attenuation of aggregation and neurotoxicity of Alzheimer's amyloid-beta peptide, ACS Appl. Mater. Interfaces. 10 (43) (2018) 36615–36621.
[40] J. Wang, Y. Gu, X. Liu, Y. Fan, Y. Zhang, C. Yi, et al., Near-infrared photothermally enhanced photo-oxygenation for inhibition of amyloid-beta aggregation based on RVG-conjugated porphyrinic metal-organic framework and indocyanine green nanoplatform, Int. J. Mol. Sci. 23 (18) (2022).
[41] G. Cheng, A. Xie, Z. Yan, X. Zhu, Y. Song, T. Chen, Nanomedicines for Alzheimer's disease: Therapies based on pathological mechanisms, Brain-x. 1 (3) (2023) e27.
[42] L. Williams, J. Larsen, Nanoparticle-mediated delivery of non-viral gene editing technology to the brain, Prog. Neurobiol. 232 (2023) 102547.
[43] M. Piccand, J. Bessa, E. Schick, C. Senn, C. Bourquin, W.F. Richter, Neonatal Immune tolerance induction to allow long-term studies with an immunogenic therapeutic monoclonal antibody in mice, AAPS J. 18 (2) (2016) 354–361.
[44] G. Pasut, F.M. Veronese, State of the art in PEGylation: the great versatility achieved after forty years of research, J. Control Release 161 (2) (2012) 461–472.
[45] R. Di Corato, F. Gazeau, C. Le Visage, D. Fayol, P. Levitz, F. Lux, et al., High-resolution cellular MRI: gadolinium and iron oxide nanoparticles for in-depth dual-cell imaging of engineered tissue constructs, ACS Nano 7 (9) (2013) 7500–7512.
[46] J. Cheng, H. Huang, Y. Chen, R. Wu, Nanomedicine for diagnosis and treatment of atherosclerosis, Adv. Sci. (Weinh). 10 (36) (2023) e2304294.
[47] R. Ettlinger, U. Lachelt, R. Gref, P. Horcajada, T. Lammers, C. Serre, et al., Toxicity of metal-organic framework nanoparticles: from essential analyses to potential applications, Chem. Soc. Rev. 51 (2) (2022) 464–484.
[48] Y. Wang, H. Jin, Q. Ma, K. Mo, H. Mao, A. Feldhoff, et al., A MOF glass membrane for gas separation, Angew. Chem. Int. Ed. Engl. 59 (11) (2020) 4365–4369.
[49] C. Wang, Y. Sun, L. Li, R. Krishna, T. Ji, S. Chen, et al., Titanium-oxo cluster assisted fabrication of a defect-rich Ti-MOF membrane showing versatile gas-separation performance, Angew. Chem. Int. Ed. Engl. 61 (26) (2022) e202203663.
[50] H. Liu, Y. Xu, L. Li, X. Dai, Deciphering the underlying mechanism of MOF-808-based abiotic catalysis enhancing biodegradability of waste activated sludge: Insights from the effects on bioconversion of extracellular organic substances into methane, Sci. Total Environ. 849 (2022) 157855.
[51] I. Christodoulou, P. Lyu, C.V. Soares, G. Patriarche, C. Serre, G. Maurin, et al., Nanoscale iron-based metal-organic frameworks: incorporation of functionalized drugs and degradation in biological media, Int. J. Mol. Sci. 24 (4) (2023).
[52] M. Ahmadi, S.M. Ayyoubzadeh, F. Ghorbani-Bidkorbeh, S. Shahhosseini, S. Dadashzadeh, E. Asadian, et al., An investigation of affecting factors on MOF

characteristics for biomedical applications: A systematic review, Heliyon. 7 (4) (2021) e06914.
[53] S. Li, L. Tan, X. Meng, Nanoscale metal-organic frameworks: synthesis, biocompatibility, imaging applications, and thermal and dynamic therapy of tumors, Adv. Funct. Mater. 30 (13) (2020) 1908924.
[54] L.L. Xiong, L.L. Xue, R.L. Du, R.Z. Niu, L. Chen, J. Chen, et al., Single-cell RNA sequencing reveals B cell-related molecular biomarkers for Alzheimer's disease, Exp. Mol. Med. 53 (12) (2021) 1888–1901.
[55] J. Chen, K. Shen, Y. Li, Greening the processes of metal-organic framework synthesis and their use in sustainable catalysis, ChemSusChem 10 (16) (2017) 3165–3187.
[56] P. Kumar, B. Anand, Y.F. Tsang, K.H. Kim, S. Khullar, B. Wang, Regeneration, degradation, and toxicity effect of MOFs: opportunities and challenges, Environ. Res. 176 (2019) 108488.
[57] T. Baati, L. Njim, F. Neffati, A. Kerkeni, M. Bouttemi, R. Gref, et al., In depth analysis of the in vivo toxicity of nanoparticles of porous iron(iii) metal–organic frameworks, Chem.. Sci. 4 (4) (2013) 1597–1607.
[58] S. Rojas, T. Baati, L. Njim, L. Manchego, F. Neffati, N. Abdeljelil, et al., Metal-organic frameworks as efficient oral detoxifying agents, J. Am. Chem. Soc. 140 (30) (2018) 9581–9586.
[59] S. Jiang, J. Wang, Z. Zhu, S. Shan, Y. Mao, X. Zhang, et al., The synthesis of nano bio-MOF-1 with a systematic evaluation on the biosafety and biocompatibility, Microporous Mesoporous Mater. 334 (2022) 111773.
[60] S. Deng, X. Yan, P. Xiong, G. Li, T. Ku, N. Liu, et al., Nanoscale cobalt-based metal-organic framework impairs learning and memory ability without noticeable general toxicity: First in vivo evidence, Sci. Total Environ. 771 (2021) 145063.
[61] Y. Lin, Y. Zhong, Y. Chen, L. Li, G. Chen, J. Zhang, et al., Ligand-modified erythrocyte membrane-cloaked metal-organic framework nanoparticles for targeted antitumor therapy, Mol. Pharm. 17 (9) (2020) 3328–3341.
[62] S. Lan, J. Zhang, X. Li, L. Pan, J. Li, X. Wu, et al., Low toxicity of metal-organic framework MOF-74(Co) nano-particles in vitro and in vivo, Nanomaterials (Basel) 12 (19) (2022).
[63] P.J. Jodlowski, G. Kurowski, L. Kuterasinski, M. Sitarz, P. Jelen, J. Jaskowska, et al., Cracking the chloroquine conundrum: the application of defective UiO-66 metal-organic framework materials to prevent the onset of heart defects-in vivo and in vitro, ACS Appl. Mater. Interfaces 13 (1) (2021) 312–323.
[64] I. Sifaoui, I. Pacheco-Fernandez, J.E. Pinero, V. Pino, J. Lorenzo-Morales, A simple in vivo assay using amphipods for the evaluation of potential biocompatible metal-organic frameworks, Front. Bioeng. Biotechnol. 9 (2021) 584115.
[65] J. Redfern, L. Geerts, J.W. Seo, J. Verran, L. Tosheva, L.H. Wee, Toxicity and antimicrobial properties of ZnO@ZIF-8 embedded silicone against planktonic and biofilm catheter-associated pathogens, ACS Applied Nano Materials. 1 (4) (2018) 1657–1665.
[66] M. Sajid, Toxicity of nanoscale metal organic frameworks: a perspective, Environ. Sci. Pollut. Res. Int. 23 (15) (2016) 14805–14807.
[67] C. Tamames-Tabar, D. Cunha, E. Imbuluzqueta, F. Ragon, C. Serre, M.J. Blanco-Prieto, et al., Cytotoxicity of nanoscaled metal-organic frameworks, J. Mater. Chem. B 2 (3) (2014) 262–271.
[68] N. Singh, S. Qutub, N.M. Khashab, Biocompatibility and biodegradability of metal organic frameworks for biomedical applications, J. Mater. Chem. B 9 (30) (2021) 5925–5934.
[69] K.M. de la Harpe, P.P.D. Kondiah, Y.E. Choonara, T. Marimuthu, L.C. du Toit, V. Pillay, The hemocompatibility of nanoparticles: A review of cell-nanoparticle interactions and hemostasis, Cells. 8 (10) (2019).
[70] A. Zimpel, N. Al Danaf, B. Steinborn, J. Kuhn, M. Hohn, T. Bauer, et al., Coordinative binding of polymers to metal-organic framework nanoparticles for control of interactions at the biointerface, ACS Nano 13 (4) (2019) 3884–3895.
[71] X. Ge, F. Jiang, M. Wang, M. Chen, Y. Li, J. Phipps, et al., Naringin@Metal-organic framework as a multifunctional bioplatform, ACS Appl. Mater. Interfaces 15 (1) (2023) 677–683.
[72] Y. Bian, H.Y. Chung, O.N. Bae, K.M. Lim, J.H. Chung, J. Pi, Titanium dioxide nanoparticles enhance thrombosis through triggering the phosphatidylserine exposure and procoagulant activation of red blood cells, Part. Fibre Toxicol. 18 (1) (2021) 28.
[73] D.R. Thal, J. Walter, T.C. Saido, M. Fandrich, Neuropathology and biochemistry of Abeta and its aggregates in Alzheimer's disease, Acta Neuropathol. 129 (2) (2015) 167–182.
[74] T. Iwatsubo, A. Odaka, N. Suzuki, H. Mizusawa, N. Nukina, Y. Ihara, Visualization of A beta 42(43) and A beta 40 in senile plaques with end-specific A beta monoclonals: evidence that an initially deposited species is A beta 42(43), Neuron 13 (1) (1994) 45–53.
[75] Y. Mashal, H. Abdelhady, A.K. Iyer, Comparison of tau and amyloid-beta targeted immunotherapy nanoparticles for Alzheimer's disease, Biomolecules 12 (7) (2022).
[76] T.C. Saido, T. Iwatsubo, D.M. Mann, H. Shimada, Y. Ihara, S. Kawashima, Dominant and differential deposition of distinct beta-amyloid peptide species, A beta N3(pE), in senile plaques, Neuron 14 (2) (1995) 457–466.
[77] S. Kumar, N. Rezaei-Ghaleh, D. Terwel, D.R. Thal, M. Richard, M. Hoch, et al., Extracellular phosphorylation of the amyloid beta-peptide promotes formation of toxic aggregates during the pathogenesis of Alzheimer's disease, EMBO J. 30 (11) (2011) 2255–2265.
[78] S. Kumar, O. Wirths, S. Theil, J. Gerth, T.A. Bayer, J. Walter, Early intraneuronal accumulation and increased aggregation of phosphorylated Abeta in a mouse model of Alzheimer's disease, Acta Neuropathol. 125 (5) (2013) 699–709.
[79] R.B. Maccioni, V. Cambiazo, Role of microtubule-associated proteins in the control of microtubule assembly, Physiol. Rev. 75 (4) (1995) 835–864.
[80] P. Barbier, O. Zejneli, M. Martinho, A. Lasorsa, V. Belle, C. Smet-Nocca, et al., Role of Tau as a microtubule-associated protein: structural and functional aspects, Front. Aging Neurosci. 11 (2019) 204.
[81] S. Muralidar, S.V. Ambi, S. Sekaran, D. Thirumalai, B. Palaniappan, Role of tau protein in Alzheimer's disease: The prime pathological player, Int. J. Biol. Macromol. 163 (2020) 1599–1617.
[82] S. Frank, F. Clavaguera, M. Tolnay, Tauopathy models and human neuropathology: similarities and differences, Acta Neuropathol. 115 (1) (2008) 39–53.
[83] M. Goedert, B. Falcon, F. Clavaguera, M. Tolnay, Prion-like mechanisms in the pathogenesis of tauopathies and synucleinopathies, Curr. Neurol. Neurosci. Rep. 14 (11) (2014) 495.
[84] A. Delacourte, Y. Robitaille, N. Sergeant, L. Buee, P.R. Hof, A. Wattez, et al., Specific pathological Tau protein variants characterize Pick's disease, J. Neuropathol. Exp. Neurol. 55 (2) (1996) 159–168.
[85] S. Flament, A. Delacourte, M. Verny, J.J. Hauw, F. Javoy-Agid, Abnormal Tau proteins in progressive supranuclear palsy. Similarities and differences with the neurofibrillary degeneration of the Alzheimer type, Acta Neuropathol. 81 (6) (1991) 591–596.
[86] H. Ksiezak-Reding, K. Morgan, L.A. Mattiace, P. Davies, W.K. Liu, S.H. Yen, et al., Ultrastructure and biochemical composition of paired helical filaments in corticobasal degeneration, Am. J. Pathol. 145 (6) (1994) 1496–1508.
[87] M.L. Schmidt, V. Zhukareva, K.L. Newell, V.M. Lee, J.Q. Trojanowski, Tau isoform profile and phosphorylation state in dementia pugilistica recapitulate Alzheimer's disease, Acta Neuropathol. 101 (5) (2001) 518–524.
[88] E.M. Mandelkow, E. Mandelkow, Tau in Alzheimer's disease, Trends Cell Biol. 8 (11) (1998) 425–427.
[89] J.T. Pedersen, E.M. Sigurdsson, Tau immunotherapy for Alzheimer's disease, Trends Mol. Med. 21 (6) (2015) 394–402.
[90] S.S. Kang, L. Meng, X. Zhang, Z. Wu, A. Mancieri, B. Xie, et al., Tau modification by the norepinephrine metabolite DOPEGAL stimulates its pathology and propagation, Nat. Struct. Mol. Biol. 29 (4) (2022) 292–305.
[91] S.A. Yuzwa, A.H. Cheung, M. Okon, L.P. McIntosh, D.J. Vocadlo, O-GlcNAc modification of tau directly inhibits its aggregation without perturbing the conformational properties of tau monomers, J. Mol. Biol. 426 (8) (2014) 1736–1752.
[92] S.A. Yuzwa, X. Shan, M.S. Macauley, T. Clark, Y. Skorobogatko, K. Vosseller, et al., Increasing O-GlcNAc slows neurodegeneration and stabilizes tau against aggregation, Nat. Chem. Biol. 8 (4) (2012) 393–399.
[93] I.C. Stancu, B. Vasconcelos, L. Ris, P. Wang, A. Villers, E. Peeraer, et al., Templated misfolding of Tau by prion-like seeding along neuronal connections impairs neuronal network function and associated behavioral outcomes in Tau transgenic mice, Acta Neuropathol. 129 (6) (2015) 875–894.
[94] F. Clavaguera, H. Akatsu, G. Fraser, R.A. Crowther, S. Frank, J. Hench, et al., Brain homogenates from human tauopathies induce tau inclusions in mouse brain, PNAS 110 (23) (2013) 9535–9540.
[95] M. Jucker, L.C. Walker, Pathogenic protein seeding in Alzheimer disease and other neurodegenerative disorders, Ann. Neurol. 70 (4) (2011) 532–540.
[96] H. Braak, E. Braak, Evolution of the neuropathology of Alzheimer's disease, Acta Neurol. Scand. Suppl. 165 (1996) 3–12.
[97] G. Zhang, Z. Wang, H. Hu, M. Zhao, L. Sun, Microglia in Alzheimer's disease: a target for therapeutic intervention, Front. Cell. Neurosci. 15 (2021) 749587.
[98] S. Krasemann, C. Madore, R. Cialic, C. Baufeld, N. Calcagno, R. El Fatimy, et al., The TREM2-APOE pathway drives the transcriptional phenotype of dysfunctional microglia in neurodegenerative diseases, Immunity 47 (3) (2017), 566-81 e9.
[99] H. Keren-Shaul, A. Spinrad, A. Weiner, O. Matcovitch-Natan, R. Dvir-Szternfeld, T.K. Ulland, et al., A Unique microglia type associated with restricting development of Alzheimer's disease, Cell 169 (7) (2017), 1276-90 e17.
[100] Y. Hu, G.L. Fryatt, M. Ghorbani, J. Obst, D.A. Menassa, M. Martin-Estebane, et al., Replicative senescence dictates the emergence of disease-associated microglia and contributes to Abeta pathology, Cell Rep. 35 (10) (2021) 109228.
[101] V. Lau, L. Ramer, M.E. Tremblay, An aging, pathology burden, and glial senescence build-up hypothesis for late onset Alzheimer's disease, Nat. Commun. 14 (1) (2023) 1670.
[102] L. Dai, Y. Shen, Insights into T-cell dysfunction in Alzheimer's disease, Aging Cell 20 (12) (2021) e13511.
[103] R. Das, S. Chinnathambi, Microglial priming of antigen presentation and adaptive stimulation in Alzheimer's disease, Cell. Mol. Life Sci. 76 (19) (2019) 3681–3694.
[104] C. Zhang, B. Raveney, F. Takahashi, T.W. Yeh, H. Hohjoh, T. Yamamura, et al., Pathogenic microglia orchestrate neurotoxic properties of eomes-expressing helper T cells, Cells 12 (6) (2023).
[105] L. van Olst, L. Coenen, J.M. Nieuwland, C. Rodriguez-Mogeda, N.M. de Wit, A. Kamermans, et al., Crossing borders in Alzheimer's disease: A T cell's perspective, Adv. Drug Deliv. Rev. 188 (2022) 114398.
[106] S.E. Marsh, E.M. Abud, A. Lakatos, A. Karimzadeh, S.T. Yeung, H. Davtyan, et al., The adaptive immune system restrains Alzheimer's disease pathogenesis by modulating microglial function, PNAS 113 (9) (2016) E1316–E1325.
[107] K. Kim, X. Wang, E. Ragonnaud, M. Bodogai, T. Illouz, M. DeLuca, et al., Therapeutic B-cell depletion reverses progression of Alzheimer's disease, Nat. Commun. 12 (1) (2021) 2185.
[108] Y.Y. Syed, Sodium oligomannate: first approval, Drugs 80 (4) (2020) 441–444.
[109] X. Wang, G. Sun, T. Feng, J. Zhang, X. Huang, T. Wang, et al., Sodium oligomannate therapeutically remodels gut microbiota and suppresses gut

bacterial amino acids-shaped neuroinflammation to inhibit Alzheimer's disease progression, Cell Res. 29 (10) (2019) 787–803.
[110] T. Doifode, V.V. Giridharan, J.S. Generoso, G. Bhatti, A. Collodel, P.E. Schulz, et al., The impact of the microbiota-gut-brain axis on Alzheimer's disease pathophysiology, Pharmacol. Res. 164 (2021) 105314.
[111] S. Poole, S.K. Singhrao, L. Kesavalu, M.A. Curtis, S. Crean, Determining the presence of periodontopathic virulence factors in short-term postmortem Alzheimer's disease brain tissue, J. Alzheimers Dis. 36 (4) (2013) 665–677.
[112] S.S. Dominy, C. Lynch, F. Ermini, M. Benedyk, A. Marczyk, A. Konradi, et al., Porphyromonas gingivalis in Alzheimer's disease brains: Evidence for disease causation and treatment with small-molecule inhibitors, Sci. Adv. 5 (1) (2019) eaau3333.
[113] Y.J. Kim, S.M. Kim, D.H. Jeong, S.K. Lee, M.E. Ahn, O.H. Ryu, Associations between metabolic syndrome and type of dementia: analysis based on the National Health Insurance Service database of Gangwon province in South Korea, Diabetol. Metab. Syndr. 13 (1) (2021) 4.
[114] X. Huang, Y.J. Wang, Y. Xiang, Bidirectional communication between brain and visceral white adipose tissue: Its potential impact on Alzheimer's disease, EBioMedicine 84 (2022) 104263.
[115] J. Han, M. Zhang, G. Chen, Y. Zhang, Q. Wei, Y. Zhuo, et al., Ferrocene covalently confined in porous MOF as signal tag for highly sensitive electrochemical immunoassay of amyloid-beta, J. Mater. Chem. B 5 (42) (2017) 8330–8336.
[116] J. Fang, G. Zhao, X. Dong, X. Li, J. Miao, Q. Wei, et al., Ultrasensitive electrochemiluminescence immunosensor for the detection of amyloid-beta proteins based on resonance energy transfer between g-C(3)N(4) and Pd NPs coated NH(2)-MIL-53, Biosens. Bioelectron. 142 (2019) 111517.
[117] J. Miao, X. Li, Y. Li, X. Dong, G. Zhao, J. Fang, et al., Dual-signal sandwich electrochemical immunosensor for amyloid beta-protein detection based on Cu-Al (2)O(3)-g-C(3)N(4)-Pd and UiO-66@PANI-MB, Anal. Chim. Acta 1089 (2019) 48–55.
[118] G. Zhao, Y. Wang, X. Li, Q. Yue, X. Dong, B. Du, et al., Dual-quenching electrochemiluminescence strategy based on three-dimensional metal-organic frameworks for ultrasensitive detection of amyloid-beta, Anal. Chem. 91 (3) (2019) 1989–1996.
[119] X. Dong, G. Zhao, X. Li, J. Fang, J. Miao, Q. Wei, et al., Electrochemiluminescence immunosensor of "signal-off" for beta-amyloid detection based on dual metal-organic frameworks, Talanta 208 (2020) 120376.
[120] Y. Gao, X. Fan, X. Zhang, Q. Guan, Y. Xing, W. Song, Switchable multiplex photoelectrochemical immunoassay of abeta(42) and abeta(40) Based on a pH-responsive i-motif probe and pyrene-based MOF photocathode, Anal. Chem. 94 (17) (2022) 6621–6627.
[121] H.X. Ren, Q. Zhong, Y.B. Miao, X.W. Wen, G.Y. Wu, H.L. Wang, et al., A label-free reusable aptasensor for Alzheimer's disease, Mikrochim. Acta 187 (9) (2020) 515.
[122] L. Yin, Y. Wang, R. Tan, H. Li, Y. Tu, Determination of beta-amyloid oligomer using electrochemiluminescent aptasensor with signal enhancement by AuNP/MOF nanocomposite, Mikrochim. Acta 188 (2) (2021) 53.
[123] Y.B. Miao, Q. Zhong, H.X. Ren, Engineering a thermostable biosensor based on biomimetic mineralization HRP@Fe-MOF for Alzheimer's disease, Anal. Bioanal. Chem. 414 (29–30) (2022) 8331–8339.
[124] Y. Wang, Y. Zhang, H. Sha, X. Xiong, N. Jia, Design and biosensing of a ratiometric electrochemiluminescence resonance energy transfer aptasensor between a g-C(3)N(4) nanosheet and Ru@MOF for amyloid-beta protein, ACS Appl. Mater. Interfaces 11 (40) (2019) 36299–36306.
[125] H.X. Ren, Y.B. Miao, Y. Zhang, An aptamer based fluorometric assay for amyloid-beta oligomers using a metal-organic framework of type Ru@MIL-101(Al) and enzyme-assisted recycling, Mikrochim. Acta 187 (2) (2020) 114.
[126] X. Wang, L. Li, X. Gu, B. Yu, M. Jiang, Switchable electrochemical aptasensor for amyloid-beta oligomers detection based on triple helix switch coupling with AuNPs@CuMOF labeled signaling displaced-probe, Mikrochim. Acta 188 (2) (2021) 49.
[127] X. Yan, Y. Pan, L. Ji, J. Gu, Y. Hu, Y. Xia, et al., Multifunctional metal-organic framework as a versatile nanoplatform for abeta oligomer imaging and chemo-photothermal treatment in living cells, Anal. Chem. 93 (41) (2021) 13823–13834.
[128] X. Zhou, S. Wang, C. Zhang, Y. Lin, J. Lv, S. Hu, et al., Colorimetric determination of amyloid-beta peptide using MOF-derived nanozyme based on porous ZnO-Co (3)O(4) nanocages, Mikrochim. Acta 188 (2) (2021) 56.
[129] W.K. Fang, L. Liu, L.L. Zhang, D. Liu, Y. Liu, H.W. Tang, Detection of amyloid beta oligomers by a fluorescence ratio strategy based on optically trapped highly doped upconversion nanoparticles-SiO(2)@metal-organic framework microspheres, Anal. Chem. 93 (36) (2021) 12447–12455.
[130] X.Z. Wang, J. Du, N.N. Xiao, Y. Zhang, L. Fei, J.D. LaCoste, et al., Driving force to detect Alzheimer's disease biomarkers: application of a thioflavine T@Er-MOF ratiometric fluorescent sensor for smart detection of presenilin 1, amyloid beta-protein and acetylcholine, Analyst 145 (13) (2020) 4646–4663.
[131] Y. Zhou, Z. Huang, J. Liu, H. Dong, Y. Zhang, M. Xu, et al., Tyrosine-conjugation method for evaluating BACE1 activity based on silver nanoparticles/metal-organic framework composites as electrochemical tags, Chemistry (2023) e202300450.
[132] J. Xiao, S.S. Yang, J.X. Wu, H. Wang, X. Yu, W. Shang, et al., Highly selective capture of monophosphopeptides by two-dimensional metal-organic framework nanosheets, Anal. Chem. 91 (14) (2019) 9093–9101.
[133] X. Lin, E. Shuang, X. Chen, Metal-organic framework/3,3',5,5'-tetramethylbenzidine based multidimensional spectral array platform for sensitive discrimination of protein phosphorylation, J. Colloid Interface Sci. 602 (2021) 513–519.
[134] A.H. Valekar, B.S. Batule, M.I. Kim, K.H. Cho, D.Y. Hong, U.H. Lee, et al., Novel amine-functionalized iron trimesates with enhanced peroxidase-like activity and their applications for the fluorescent assay of choline and acetylcholine, Biosens. Bioelectron. 100 (2018) 161–168.
[135] F. Wang, M. Liu, X. Niu, L. Xia, F. Qu, Dextran-assisted ultrasonic exfoliation of two-dimensional metal-organic frameworks to evaluate acetylcholinesterase activity and inhibitor screening, Anal. Chim. Acta 1243 (2023) 340815.
[136] Y. Wang, Y. Xue, Q. Zhao, S. Wang, J. Sun, X. Yang, Colorimetric assay for acetylcholinesterase activity and inhibitor screening based on metal-organic framework nanosheets, Anal. Chem. 94 (47) (2022) 16345–16352.
[137] Y.B. Hao, Z.S. Shao, C. Cheng, X.Y. Xie, J. Zhang, W.J. Song, et al., Regulating fluorescent aptamer-sensing behavior of zeolitic imidazolate framework (ZIF-8) platform via lanthanide ion doping, ACS Appl. Mater. Interfaces 11 (35) (2019) 31755–31762.
[138] P. Zhang, C. Tan, Cross-reactive fluorescent sensor array for discrimination of amyloid beta aggregates, Anal. Chem. 94 (14) (2022) 5469–5473.
[139] T.H. Ferreira-Vieira, I.M. Guimaraes, F.R. Silva, F.M. Ribeiro, Alzheimer's disease: targeting the cholinergic system, Curr. Neuropharmacol. 14 (1) (2016) 101–115.
[140] L. Yang, Y. Chen, Z. Jia, X. Yuan, J. Liu, Electrostatic assembly of gold nanoparticle and metal-organic framework nanoparticles attenuates amyloid beta aggregate-mediated neurotoxicity, J. Mater. Chem. B (2023).
[141] Y. Su, Y. Huang, Q. Kou, L. Lu, H. Jiang, X. Li, et al., Study on the role of an erythrocyte membrane-coated nanotheranostic system in targeted immune regulation of Alzheimer's disease, Adv. Sci. (Weinh) (2023) e2301361.
[142] D. Yu, M. Ma, Z. Liu, Z. Pi, X. Du, J. Ren, et al., MOF-encapsulated nanozyme enhanced siRNA combo: Control neural stem cell differentiation and ameliorate cognitive impairments in Alzheimer's disease model, Biomaterials 255 (2020) 120160.
[143] S. Kwiatkowski, B. Knap, D. Przystupski, J. Saczko, E. Kedzierska, K. Knap-Czop, et al., Photodynamic therapy - mechanisms, photosensitizers and combinations, Biomed. Pharmacother. 106 (2018) 1098–1107.
[144] J.R. Jagdeo, L.E. Adams, N.I. Brody, D.M. Siegel, Transcranial red and near infrared light transmission in a cadaveric model, PLoS One 7 (10) (2012) e47460.
[145] X. Li, J.F. Lovell, J. Yoon, X. Chen, Clinical development and potential of photothermal and photodynamic therapies for cancer, Nat. Rev. Clin. Oncol. 17 (11) (2020) 657–674.
[146] X. Li, Z. Han, T. Wang, C. Ma, H. Li, H. Lei, et al., Cerium oxide nanoparticles with antioxidative neurorestoration for ischemic stroke, Biomaterials 291 (2022) 121904.
[147] R. Kiss, G. Csizmadia, K. Solti, A. Keresztes, M. Zhu, M. Pickhardt, et al., Structural basis of small molecule targetability of monomeric tau protein, ACS Chem. Nerosci. 9 (12) (2018) 2997–3006.
[148] J.V. Pluvinage, M.S. Haney, B.A.H. Smith, J. Sun, T. Iram, L. Bonanno, et al., CD22 blockade restores homeostatic microglial phagocytosis in ageing brains, Nature 568 (7751) (2019) 187–192.
[149] M. Stazi, S. Lehmann, M.S. Sakib, T. Pena-Centeno, L. Buschgens, A. Fischer, et al., Long-term caffeine treatment of Alzheimer mouse models ameliorates behavioural deficits and neuron loss and promotes cellular and molecular markers of neurogenesis, Cell. Mol. Life Sci. 79 (1) (2021) 55.